J. PharmTechNova. Volume: 01; Issue: 02; Year: 26; Pages: 73-107
DOI: https://doi.org/10.66220/75p78209

ISSN: 3139-9258

Journal of PharmTechNova (JPTN)
https://pharmtechnova.com/index.php/jptn

Research Article

Development, Optimization and Evaluation of Naproxen Amorphous ASDs Tablets for Enhanced Solubility and Dissolution Using Hydrophilic Polymers

Parvez Musharraf Khan Ayyub Khan*, Mohd Bilal Sufi

Department of Pharmaceutics, New Montfort Institute of Pharmacy, Ashti, Peth Ahmadpur, Maharashtra 442202, India.
*Corresponding author: parvezmusharrafk@gmail.com

Article info:

Submitted: 14/07/2026
Revised: 19/08/2026
Accepted: 19/08/2026
Published: 26/08/2026
Manuscript ID: 00018
Subject: Pharmaceutical Technology and Drug Development

Keywords:
Amorphous solid dispersion; Dissolution study; Factorial design; Naproxen; Response surface methodology; Solubility enhancement; Solvent evaporation; Tablet formulation.

Abstract:
Naproxen is a widely prescribed non-steroidal anti-inflammatory drug (NSAID) belonging to Biopharmaceutical Classification System (BCS) Class II, exhibiting high permeability but poor aqueous solubility, which limits its dissolution rate and oral bioavailability. The present study aimed to develop, optimize, and evaluate amorphous solid dispersions (ASDs) of naproxen using hydrophilic polymers to improve its solubility and dissolution characteristics. Preformulation studies including melting point determination, Fourier Transform Infrared Spectroscopy (FTIR) spectroscopy, differential scanning calorimetry (DSC), powder X-ray diffraction (PXRD), UV spectrophotometric analysis, and solubility studies confirmed the identity, purity, and crystalline nature of naproxen. ASDs were prepared by the solvent evaporation method using PVP K30, PEG 6000, HPMC E5, and Poloxamer 188 individually and in combinations. Preliminary screening demonstrated that PVP K30 exhibited the highest solubility enhancement, while the combination of PVP K30 and PEG 6000 showed synergistic improvement. Formulation variables were optimized using response surface methodology (RSM) based on a factorial design with polymer concentration and ethanol volume as independent variables. The optimized formulation (F6) exhibited a production yield of 95.40%, drug content of 86.23%, and 95.68% cumulative drug release within 60 minutes. FTIR and DSC analyses confirmed the absence of significant drug–polymer interactions and indicated successful formation of the ASDs. The optimized dispersion was compressed into tablets that demonstrated acceptable pre- and post-compression characteristics, including hardness, friability, weight variation, and drug content. The tablet formulation released 96.23% of drug within 60 minutes and followed the Korsmeyer–Peppas kinetic model, suggesting anomalous drug release behavior. Accelerated stability studies conducted for three months revealed no significant changes in physicochemical properties or dissolution profile. The findings demonstrate that the developed ASDs tablet effectively enhances the solubility and dissolution of naproxen and represents a promising strategy for improving its oral bioavailability.

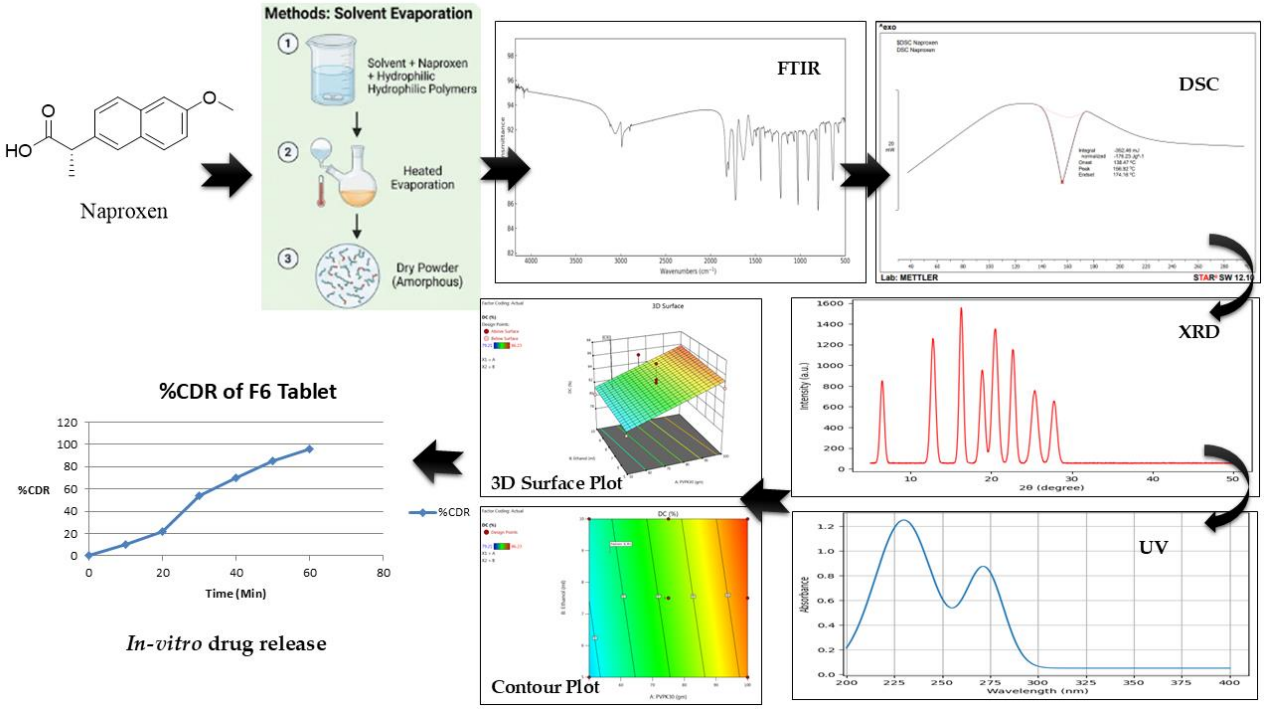
DOI: https://doi.org/10.66220/75p78209 ISSN: 3139-9258

How to Cite this article: P.M.K.A. Khan, M.B. Sufi. Development, Optimization and Evaluation of Naproxen Amorphous ASDs Tablets for Enhanced Solubility and Dissolution Using Hydrophilic Polymers. *J. PharmTechNova.* **2026**, 01 [02], 73-107. DOI: https://doi.org/10.66220/75p78209

©2026 The authors

This is an Open Access article distributed under the terms of the Creative Commons Attribution (CC BY NC), which permits unrestricted use, distribution, and reproduction in any medium, as long as the original authors and source are cited. No permission is required from the authors or the publishers. (https://creativecommons.org/licenses/by-nc/4.0/)

Graphical Abstract



1. Introduction

Naproxen is a widely used non-steroidal anti-inflammatory drug (NSAID) belonging to the propionic acid class and is extensively prescribed for rheumatoid arthritis, osteoarthritis, ankylosing spondylitis, acute musculoskeletal disorders, dysmenorrhea, gout, and various inflammatory conditions. It exerts its pharmacological action by inhibiting cyclooxygenase (COX) enzymes, thereby reducing the synthesis of prostaglandins responsible for pain, inflammation, and fever. Owing to its potent anti-inflammatory and analgesic activities, naproxen is one of the most frequently prescribed oral NSAIDs. However, its therapeutic effectiveness is often limited by poor aqueous solubility, which restricts its dissolution in gastrointestinal fluids and consequently delays drug absorption following oral administration [1–3].

According to the Biopharmaceutics Classification System (BCS), naproxen is classified as a Class II drug, characterized by high permeability and low aqueous solubility. The dissolution rate is the primary factor governing oral absorption and bioavailability of BCS Class II drugs. Inadequate dissolution results in a delayed onset of therapeutic action, variable plasma drug concentrations, and inconsistent clinical efficacy. Therefore, enhancing the dissolution characteristics of poorly water-soluble drugs has become an important objective in modern pharmaceutical formulation research to achieve improved bioavailability and therapeutic performance. [4,5].

Several formulation approaches have been explored to overcome the poor solubility of hydrophobic drugs in water. These include particle size reduction, crystal engineering, inclusion complex formation, lipid-

DOI: https://doi.org/10.66220/75p78209 ISSN: 3139-9258

based drug delivery systems, nanotechnology-based formulations, co-crystals, self-emulsifying systems, and amorphous solid dispersion (ASDs) technology. Among these strategies, ASDs have emerged as one of the most effective and commercially successful techniques for improving the apparent solubility and dissolution rates of poorly soluble drug molecules. In this approach, the drug is dispersed within a polymeric carrier in an amorphous or molecularly dispersed state, leading to reduced crystallinity, increased surface area, enhanced wettability, and improved dissolution. The conversion of a crystalline drug into an amorphous form also increases its free energy, thereby facilitating its rapid dissolution in biological fluids.

The performance of ASDs is strongly influenced by the selection of suitable hydrophilic carriers and preparation method. Hydrophilic polymers are widely employed because they improve the wetting of drug particles, inhibit recrystallization, stabilize the amorphous form during storage, and maintain supersaturation after dissolution [6,7]. Similarly, the manufacturing technique plays a critical role in determining the physicochemical characteristics and stability of the ASDs. Various preparation methods, including solvent evaporation, melting, spray drying, hot-melt extrusion, freeze drying, and supercritical fluid processing, have been investigated for the development of ASDs, each offering specific advantages depending on the physicochemical properties of the drug and carrier used.

The quality and performance of pharmaceutical formulations can be further enhanced through systematic optimization using a statistical experimental design. Response Surface Methodology (RSM) and Design of Experiments (DoE) are efficient tools for evaluating the influence of formulation and process variables, minimizing experimental trials, and identifying optimal formulation conditions [8–10]. In addition, comprehensive physicochemical characterization and dissolution studies are essential for understanding drug–carrier interactions, solid-state properties, formulation performance and stability during storage.

Therefore, the present study aimed to develop, optimize, and evaluate amorphous ASDs tablets of naproxen to improve its solubility and dissolution characteristics. This study also aimed to optimize the formulation using an appropriate statistical design and comprehensively characterize the developed formulation to establish an effective oral dosage system with enhanced pharmaceutical performance.

2. Materials and Methods

2.1 Materials

2.1.1 Chemicals and Reagents

Naproxen was used as the active pharmaceutical ingredient in the present investigation. Hydrophilic polymers, such as Polyvinylpyrrolidone K30 (PVP K30), Polyethylene Glycol 6000 (PEG 6000), Hydroxypropyl Methylcellulose (HPMC E5), and poloxamer 188, were used as carriers for the preparation of ASDs. Ethanol was employed as a solvent for the solvent evaporation method because of its ability to dissolve both drugs and polymers effectively. Distilled water and buffer solutions of pH 1.2, 6.8, and 7.4 were used for solubility studies, calibration curve preparation, and dissolution studies, respectively. Potassium bromide (KBr) was used for Fourier-transform infrared (FTIR) spectroscopy, and liquid paraffin was used for melting point determination. All chemicals and reagents used in this study were of analytical grade and used as received without further purification.

2.1.2 Instruments and Apparatus

The instruments used in the study included a UV–visible spectrophotometer (Shimadzu UV-1800PC, Japan) for analytical measurements and calibration studies, and an FTIR spectrophotometer (Shimadzu 8400S, Japan) for drug identification and compatibility studies. Differential Scanning Calorimetry (DSC) was performed using a Mettler DSC 1 Star System (Mettler-Toledo, Switzerland) to study the thermal behavior. Powder X-ray diffraction analysis was performed using an X-ray diffractometer with a Cu target. A motorized pellet press (Kimaya Engineers, India) was used to prepare the KBr pellets.

DOI: https://doi.org/10.66220/75p78209 ISSN: 3139-9258

Additional apparatus included an orbital shaking incubator for solubility studies, dissolution apparatus (USP Type II) for in vitro drug release studies, vacuum oven for drying ASDs, and water bath for solvent evaporation. Other common laboratory equipment, such as an analytical balance, pH meter, sonicator, funnel, graduated cylinders, and glassware, were used throughout the study.

2.2 Methods

2.2.1 Preformulation study

Preformulation studies are the first and most important step in the development of pharmaceutical formulations. They involve the evaluation of the physicochemical properties of the drug alone and in combination with excipients to support the development of stable and effective dosage forms.

Identification and Confirmation of Drug

Drug identification and confirmation were performed by determining the melting point using the capillary method, followed by characterization using differential scanning calorimetry (DSC), Fourier-transform infrared (FTIR) spectroscopy, and Powder X-ray Diffraction (P-XRD) analysis.

Melting Point Method

The melting point of the drug was determined as an initial step to verify its identity and to assess its purity. A small quantity of the drug was packed into a capillary tube sealed at one end, which was then secured alongside a thermometer and immersed in a liquid-paraffin bath. The sample was heated gradually, and the temperatures corresponding to the beginning and completion of melting were recorded as the melting point range [11,12].

FTIR Spectroscopy

FTIR spectroscopy was performed to confirm the identity of the drug and to identify its characteristic functional groups. The drug sample was finely powdered and uniformly blended with potassium bromide (KBr) at a ratio of 1:100 (w/w). The mixture was compressed into transparent pellets using a motorized pellet press (Kimaya Engineers, India) under a pressure of 10–12 metric tonnes. The prepared pellets were analyzed over a spectral range of 4000–400 cm^{-1} using an FTIR spectrometer (Shimadzu 8400S, Japan), and the corresponding infrared spectra were recorded [13–15].

DSC

DSC was performed to evaluate the thermal behavior and confirm the crystalline nature of the drug. An accurately weighed sample of naproxen was placed in a perforated aluminum pan and analyzed using a DSC instrument (Mettler DSC 1 Star System, Mettler-Toledo, Switzerland). The sample was heated from 30 to 350°C at a constant heating rate of 10°C/min under a nitrogen atmosphere maintained at a flow rate of 20 mL/min, and the resulting thermogram was recorded [16,17].

XRD

P-XRD analysis was performed to investigate the crystalline characteristics of the drugs. The diffraction pattern was recorded using an X-ray diffractometer equipped with a copper (Cu) target operated at 40 kV. The sample was scanned over a diffraction angle (2θ) range of 10°–50° at a scanning rate of 3°/min, and the obtained diffractogram was used to assess the crystallinity of the drug [18,19].

2.2.2 Analytical methods

Standard Calibration Curves

Standard calibration curves of naproxen were established in ethanol, pH 1.2 buffer, pH 6.8 buffer, and pH 7.4 buffer using UV–visible spectrophotometry. A stock solution containing 100 mg of naproxen was

DOI: https://doi.org/10.66220/75p78209 ISSN: 3139-9258

prepared by initially dissolving the drug in 5 mL of the respective medium and making up the volume to 100 mL with the same solvent. Appropriate serial dilutions were prepared to obtain concentration ranges of 5–30 µg/mL in ethanol, 10–40 µg/mL in pH 1.2 buffer, 5–30 µg/mL in pH 6.8 buffer, and 2–20 µg/mL in pH 7.4 buffer. Each solution was scanned to determine the maximum absorption wavelength (λmax), which was observed at 271 nm in all the media. The absorbance of the prepared dilutions was measured at 271 nm, and calibration plots were constructed by plotting the concentration against the absorbance in accordance with Beer–Lambert's law. The resulting standard calibration curves were subsequently employed for the quantitative estimation of naproxen during in vitro dissolution studies [20–23].

2.2.3 Solubility Determination

The equilibrium solubility of naproxen was determined in ethanol, distilled water, and buffers at pH 1.2, 6.8, and 7.4 to evaluate its solubility profile. An excess amount of drug was added to 10 mL of each medium in sealed glass vials and shaken in an orbital incubator at 37 ± 0.5°C for 24 h, followed by equilibration at the same temperature for an additional 12 h. The saturated solutions were filtered through a 0.45 µm membrane filter, and the drug concentration in the filtrate was quantified by UV–visible spectrophotometry at 271 nm using the corresponding calibration curve. The solubility of naproxen in each medium was calculated [22,24].

2.2.4 Preformulation Drug–Polymer Compatibility Assessment

Drug–polymer compatibility was evaluated using FT-IR spectroscopy and DSC. FTIR analysis was performed on the pure drug, individual excipients, and their physical mixture by preparing potassium bromide (KBr) pellets in a 1:100 (sample, w/w) ratio. The pellets were compressed under 10–12 metric tons of pressure using a motorized pellet press (Kimaya Engineers, India) and scanned over the spectral range of 4000–400 cm^{-1} using an FTIR spectrometer (Shimadzu 8400S, Japan) to detect any possible drug–excipient interactions [13–15]. Thermal compatibility was further assessed by DSC using a Mettler DSC 1 Star System (Mettler-Toledo, Switzerland). Accurately weighed samples of the drug, excipients, and their physical mixtures were sealed in perforated aluminum pans and heated from 30 to 350°C at a rate of 10°C/min under a nitrogen atmosphere maintained at a flow rate of 20 mL/min. The obtained thermograms were compared to identify any changes in the thermal behavior that were indicative of incompatibility [16,17].

2.2.5 Screening of Polymers for each method

Selection of method for the formulation of ASDs

The solvent evaporation technique was selected for the preparation of ASDs because of its simplicity, ease of scale-up, and ability to achieve efficient solvent removal with a high product recovery. This method also facilitates the uniform dispersion of the drug within the polymeric matrix, making it suitable for the development of stable ASDs.

2.2.6 Primary Studies

Selection of polymers for the formulation of binary, ternary and quaternary ASDs

The selection of suitable hydrophilic polymers is a critical step in developing ASDs, as polymer characteristics and drug-to-polymer ratios significantly influence drug solubility, stability, and overall formulation performance (25,26). Based on literature reports, PVP K30, PEG 6000, HPMC E5, and Poloxamer 188 were selected as the carrier polymers for screening. Binary ASDs of Naproxen with each polymer were initially prepared using the solvent evaporation method to identify the most effective carriers for solubility enhancement. The selected polymers were subsequently employed to formulate ternary and quaternary ASDs. The compositions of the prepared formulations are presented in Table 1.

Table 1. ASDs of drug for screening of polymer

Batch Code	Polymer	Drug: Polymer ratio	Preparation Technique
1	PVPK30	1:1	Solvent Evaporation Method

2	PVPK30	1:3
3	PVPK30	1:5
4	HPMC E5	1:1
5	HPMC E5	1:3
6	HPMC E5	1:5
7	PEG6000	1:1
8	PEG6000	1:3
9	PEG6000	1:5
10	Poloxamer 188	1:1
11	Poloxamer 188	1:3
12	Poloxamer 188	1:5
13	PVPK30/PEG6000	1:1:1
14	HPMC E5/PEG6000	1:1:1
15	PVPK30/HPMCE5	1:1:1

2.2.7 Preparation of ASDs of drug using different concentrations of each polymer

Solvent evaporation

ASDs were prepared using a solvent evaporation technique. The required amount of naproxen was dissolved in ethanol, after which the selected polymer was gradually incorporated with continuous stirring to obtain a uniform solution. The solvent was evaporated in a water bath until a solid mass was formed, which was subsequently dried in a vacuum oven to remove any residual solvent. The dried product was pulverized, passed through an appropriate sieve, and stored in an airtight container in a desiccator until further characterization was performed.

2.2.8 Evaluation of ASDs

Phase solubility study

Phase solubility studies were performed according to the method described by Higuchi and Connors [27,28]. An excess amount of naproxen was added to 20 mL of aqueous polymer solutions containing 0.5–4.0% (w/v) polymer in sealed 25 mL conical flasks. The mixtures were shaken at 100 rpm in an orbital shaker maintained at 37°C for 24 h to attain equilibrium. After equilibration, the suspensions were allowed to settle, and the supernatants were filtered through Whatman Grade 1 filter paper. The filtrates were analyzed at 271 nm using a UV–visible spectrophotometer to determine the concentration of the dissolved drug. All experiments were performed in triplicate, and the results are expressed as mean values.

Saturation solubility study

The saturation solubilities of pure naproxen, physical mixtures, and ASDs were determined in distilled water, pH 1.2 buffer, and pH 6.8 buffer. An excess amount of each sample was dispersed in 20 mL of the respective medium in 25 mL conical flasks, sonicated for 10 min, and shaken at 37 ± 0.5°C for 24 h in an orbital shaker. The suspensions were then allowed to equilibrate at the same temperature, followed by filtration through a Whatman Grade 1 filter paper. The concentration of the dissolved drug in the filtrate was determined at 271 nm using a UV–visible spectrophotometer (UV-1800PC, Shimadzu, Japan). All experiments were performed in triplicate, and the mean solubility values were calculated [29–31].

2.2.9 Optimization by Factorial Design

The formulation of Naproxen ASDs was optimized using Response Surface Methodology (RSM) with a two-factor experimental design implemented in Design-Expert® software (Version 10.0.3.1, Stat-Ease Inc., USA) [32–34]. The design was employed to evaluate the individual and interactive effects of the formulation variables while minimizing the number of experiments. The amount of polymer (X_1) and the volume of ethanol

DOI: https://doi.org/10.66220/75p78209 ISSN: 3139-9258

(X_2) were selected as the independent variables based on preliminary investigations, whereas all other formulation and processing conditions were kept constant. Thirteen experimental formulations (F1–F13) were generated according to the design matrix and evaluated for drug content (%) (Y_1) and cumulative drug release at 60 min (%) (Y_2). The experimental data were fitted to a second-order polynomial model, and the generated equations were used to analyze the effects of the independent variables and identify the optimized formulation.

2.2.10 Optimization data analysis and model-validation

The experimental data obtained from the factorial design were analyzed using the Design-Expert® software (Version 10.0.3.1, Stat-Ease Inc., USA). Analysis of variance (ANOVA) was performed to evaluate the significance and adequacy of the developed polynomial model [9,35]. The relationship between the independent variables and measured responses was described using a second-order polynomial equation:

$$Y = b0 + b1X1 + b2X2 + b12X1X2 + b11X12 + b22X22 \text{ ---------- (2)}$$

where Y represents the predicted response, b_0 is the intercept, b_1 and b_2 are the coefficients of the linear terms, b_{12} is the interaction coefficient, and b_{11} and b_{22} are quadratic coefficients. X_1 and X_2 denote the coded levels of independent variables. The suitability of the model was assessed through regression analysis and ANOVA, while three-dimensional response surface and contour plots generated by the software were used to visualize the influence of formulation variables and identify the optimum formulation.

2.2.11 Evaluation of optimized ASDs formulation

Percentage yield

The percentage yield of the prepared ASDs was determined to evaluate the efficiency of the preparation process. The weight of the dried ASDs obtained after processing was compared with the total initial weight of the drug and polymer used in the formulation. The percentage yield was calculated using the following equation:

%Theoretical Yield = Practical Weight/Theoretical Weight X 100 ----- (3)

Drug content

An accurately weighed quantity of ASDs equivalent to 250 mg of naproxen was dissolved in a small volume of ethanol, and the volume was adjusted to 50 mL using the same solvent. An appropriate aliquot was diluted to 50 mL with ethanol. The resulting solution was analyzed using a UV–visible spectrophotometer at 271 nm, and the drug content was determined from the corresponding calibration curve.

***In Vitro* Dissolution Study**

The *in vitro* dissolution behavior of Naproxen ASDs was evaluated using a USP Type II dissolution apparatus containing 900 mL of pH 1.2 and pH 6.8 dissolution media maintained at 37 ± 1°C and stirred at 75 rpm. At predetermined intervals of 5 min for 60 min, 10 mL samples were withdrawn and immediately replaced with an equal volume of fresh dissolution medium to maintain sink conditions. The collected samples were analyzed at 271 nm using a UV–visible spectrophotometer, and the cumulative percentage of drug released was calculated from the corresponding calibration curve.

2.2.12 Drug-Excipients Compatibility Study

The compatibility of the optimized ASDs (F6) was assessed using FT-IR spectroscopy and DSC. For FTIR analysis, the optimized formulation was finely powdered and blended with potassium bromide (KBr) in a 1:100 (sample, w/w) ratio. The mixture was compressed into pellets under a pressure of 10–12 metric tons using a motorized pellet press (Kimaya Engineers, India) and scanned over the spectral range of 4000–400 cm^{-1} with an FTIR spectrometer (Shimadzu 8400S, Japan) to evaluate any changes in the characteristic functional groups following formulation [13–15]. Thermal compatibility was further examined using a Differential Scanning Calorimeter (DSC-PYRIS-1, PerkinElmer). The accurately weighed sample was sealed in an aluminum

DOI: https://doi.org/10.66220/75p78209 ISSN: 3139-9258

pan and heated under a dry nitrogen atmosphere at a rate of 10°C/min from room temperature to its melting point, using an empty aluminum pan as the reference. The obtained thermograms were analyzed to determine any alterations in the thermal characteristics of the optimized formulation, thereby confirming drug–excipient compatibility [16,17].

2.2.13 Evaluation of pre-compression parameters

The flow and packing characteristics of the optimized powder formulations were assessed before tablet compression. The evaluation included the angle of repose, bulk density, tapped density, Carr's compressibility index, and Hausner's ratio to determine the suitability of the powder blend for tablet manufacturing.

Angle of Repose

The angle of repose was measured using the fixed funnel method. A predetermined quantity of powder was allowed to flow freely through a funnel positioned at a fixed height on the stand. The powder formed a conical heap, and the height (h) and radius (r) were measured. The angle of repose (θ) was calculated using the following equation [36,37]:

$$\tan \theta = h/r$$

$$\theta = \tan^{-1} (h/r) \text{ ---------- (4)}$$

Bulk Density

Bulk density represents the mass of powder occupying a unit volume under untapped conditions and is influenced by particle arrangement and packing. The volume was determined by gently transferring a known weight of powder into a graduated measuring cylinder and recording the initial volume occupied by the powder [38].

Bulk density = Weight of powder / Untapped volume ---------- (5)

Tapped Density

The tapped density was determined to assess the packing behavior of the powder after mechanical consolidation. A known quantity of powder was introduced into a graduated cylinder and subjected to repeated tapping until a constant volume was reached. The final tapped volume was recorded and used for the calculations [39].

Tapped density = Weight of powder / Tapped volume ---------- (6)

Carr's Compressibility Index

Carr's index was calculated to evaluate the compressibility and flow characteristics of the powders. The was determined from the bulk and tapped density values using the following equation:

Carr's Index (%) = [(Tapped density − Bulk density) / Tapped density] × 100 ---------- (7)

Hausner's Ratio

Hausner's ratio was calculated from the relationship between the tapped density and bulk density. This parameter indicates the interparticle friction and flowability of the powder blend.

Hausner's Ratio = Tapped density / Bulk density ---------- (8)

2.2.14 Formulation of Tablet using optimized ASDs

The selected ASDs (SEM 6) were subsequently compressed into tablets containing a theoretical equivalent of 250 mg of naproxen per tablet. Lactose was incorporated as a diluent to achieve the desired tablet weight. The ASDs were thoroughly blended with talc and magnesium stearate, with magnesium stearate

incorporated at 1% w/w of the total blend, followed by compression into tablets weighing 500 mg each. For a comparative evaluation of the dissolution performance, tablets containing the plain drug without the polymer were also prepared using the same procedure [40,41].

2.2.15 Evaluation of Tablets

The prepared tablets were evaluated for various physicochemical and quality control parameters, including dimensions, mechanical strength, friability, weight uniformity, and drug content.

Diameter and Thickness

The diameter and thickness of the prepared tablets were determined to assess their dimensional uniformity. The tablet diameter was measured using a Vernier caliper, and the thickness was determined using a screw gauge. Measurements were performed for individual tablets, and the results were used to confirm the consistency among the prepared batches [42,43].

Hardness

Tablet hardness represents the resistance of a tablet to mechanical breakage or crushing. The crushing strength of the prepared tablets was determined using a Monsanto hardness tester. The hardness values were recorded in kg/cm² [42,43].

Friability

Friability was evaluated to determine the ability of the tablets to withstand abrasion and mechanical stress during their handling. Twenty tablets were accurately weighed and placed in a Roche friabilator, which was operated at 25 rpm. The apparatus was run for 4 min, during which the tablets were repeatedly subjected to impacts and abrasions. The tablets were then removed, dried, and reweighed [42,43]. The percentage weight loss was calculated using the following equation:

$$\% \text{ Friability} = [(\text{Initial weight} - \text{Final weight}) / \text{Initial weight}] \times 100 \quad (9)$$

Weight Variation

The uniformity of the tablet weight was assessed according to the Indian Pharmacopoeia (IP) procedure. Twenty tablets were randomly selected from each formulation and weighed. The mean tablet weight was calculated, and the individual tablet weights were compared with the calculated average to determine the extent of weight variation [42,43].

Drug Content

The drug content was determined to verify the uniform distribution of naproxen in the tablets. Three tablets from each formulation were individually weighed and powdered. A quantity of powder equivalent to 2 mg of naproxen was accurately transferred to a beaker containing 50 mL of ethanol. The mixture was sonicated for 15 min at 1500 rpm to ensure complete drug extraction. The resulting solution was diluted with ethanol, and its absorbance was measured at 271 nm using a UV-visible spectrophotometer. The naproxen content of the tablets was calculated from the obtained absorbance values [42,43].

***In-vitro* dissolution study**

The *in-vitro* dissolution behavior of naproxen from the prepared ASDs formulations was evaluated using a USP Type II dissolution apparatus. The study was conducted in 900 mL of dissolution medium maintained at 37 ± 1°C, with phosphate buffers of pH 1.2 and pH 6.8 used as the respective media. The apparatus was operated at 75 rpm. At predetermined intervals, 10 mL of the dissolution medium was withdrawn over 1 h, with sampling performed every 5 min. An equivalent volume of fresh dissolution medium maintained at the same temperature was immediately added after each withdrawal to maintain a constant volume. The collected samples were suitably diluted and analyzed spectrophotometrically at λmax of 271 nm using a UV-visible

DOI: https://doi.org/10.66220/75p78209 ISSN: 3139-9258

spectrophotometer. The same procedure was followed for the naproxen ASDs formulations to determine their dissolution profiles.

2.2.16 Kinetics of drug release

The dissolution data obtained from the prepared naproxen formulations were fitted to different mathematical models to elucidate the probable drug release kinetics and mechanism. The zero-order, first-order, Higuchi, and Korsmeyer–Peppas models were applied to the dissolution data, and the model with the highest coefficient of determination (R^2) was considered the best fit.

Zero-Order Model

The zero-order model describes drug release at a constant rate, wherein an approximately equal quantity of drug is released per unit of time. This model is commonly applicable to modified-release systems, including certain matrix and coated dosage forms. This relationship is expressed as [44,45]:

$$Q_t = Q_0 + K_0 t \quad \text{---------- (11)}$$

Where:
Q_t = Amount of drug released at time t
Q_0 = Initial amount of drug present in the dissolution medium
K_0 = Zero-order release constant
t = Time

First-Order Model

The first-order model describes a release pattern in which the rate of drug release depends on the amount of drug remaining in the dosage form. Consequently, the release rate decreases progressively as the drug is depleted (44,45). The equation used is:

$$\text{Log } Q_t = \text{Log } Q_0 + (K_t \times t)/2.303 \quad \text{---------- (12)}$$

Where:
Q_t = Amount of drug released at time t
Q_0 = Initial amount of drug present
K_t = First-order release constant
t = Time

Higuchi Model

The Higuchi model was employed to investigate the diffusion-controlled drug release from the matrix systems. This method is particularly useful for evaluating the release of drugs incorporated within either solid or semi-solid matrices (44,45). The general equation is as follows:

$$Q = [D(2C - C_s)C_s t]^{1/2} \quad \text{---------- (13)}$$

Where:
Q = Cumulative amount of drug released per unit area at time t
D = Diffusion coefficient of the drug
C = Initial drug concentration in the matrix
C_s = Solubility of the drug in the matrix medium
t = Time

When the diffusion coefficient and other relevant parameters remain constant during the release process, the equation can be simplified as follows:

$$Q = Kt^{1/2}$$

DOI: https://doi.org/10.66220/75p78209 ISSN: 3139-9258

A linear relationship between cumulative drug release and the square root of time indicates a diffusion-controlled release mechanism. The suitability of the model was assessed using linear regression analysis and determination of the corresponding R^2 value.

Korsmeyer–Peppas Model

The Korsmeyer–Peppas model was used to characterize the mechanism governing drug release. The model relates the cumulative fraction of drug released to the release time and provides the release exponent (n), which helps to identify the underlying release mechanism [44,45]. The mathematical expression is as follows:

$$Q = Kt^n$$

Taking logarithms on both sides gives:

$$\text{Log } Q = \text{Log } K + n \text{ Log } t \text{ ---------- (14)}$$

Where:
Q = Cumulative percentage of drug released at time t
K = Release rate constant
t = Time
n = Release exponent obtained from the slope of the plot of log Q versus log t.

2.2.17 Accelerated stability studies

The stability of the optimized naproxen ASDs tablets was evaluated for 90 days under accelerated storage conditions of 40 ± 2°C and 75 ± 5% relative humidity (RH). Samples were withdrawn at predetermined intervals and examined for changes in drug content and in vitro drug release to assess the stability and performance of the formulation throughout the study period.

3. Results and Discussion

3.1 Preformulation study

3.1.1 Identification and Confirmation of Drug

The identity and purity of naproxen were established using complementary analytical techniques, including melting point determination, DSC, FTIR, and P-XRD. The obtained results were compared with the reported characteristics of the drug to confirm its identity.

3.1.2 Melting Point Determination

The melting point of naproxen was determined using the capillary tube method with a suitable melting point apparatus. The experimentally observed melting point was compared with the standard melting point of naproxen. The obtained value was within the standard range, confirming the identity and purity of the drug. The results are shown in Table 2.

Table 2. Melting Point of Naproxen by different methods

Method	Observed Melting Point
Glass Capillary Method	155º-157ºC
Melting Point Apparatus	156º-157ºC
Differential Scanning Calorimetry	159.72ºC

3.1.3 FTIR Spectroscopy

The FTIR spectrum of naproxen exhibited characteristic absorption peaks at ~3060 cm^{-1} (O–H stretching of carboxylic acid), 2955 and 2870 cm^{-1} (aliphatic C–H stretching), a strong peak at ~1725 cm^{-1} (C=O stretching

DOI: https://doi.org/10.66220/75p78209 ISSN: 3139-9258

of the–COOH group), and bands at 1605 and 1508 cm^{-1} corresponding to the aromatic C=C stretching of the naphthalene ring. Additional peaks were observed at 1455 and 1378 cm^{-1} (C–H bending), 1265 cm^{-1} (C–O stretching of the carboxylic group), and 1170–1025 cm^{-1} (C–O and C–C stretching vibrations). The peaks in the region of 900–750 cm^{-1} indicate aromatic C–H bending, as shown in Figure 1.

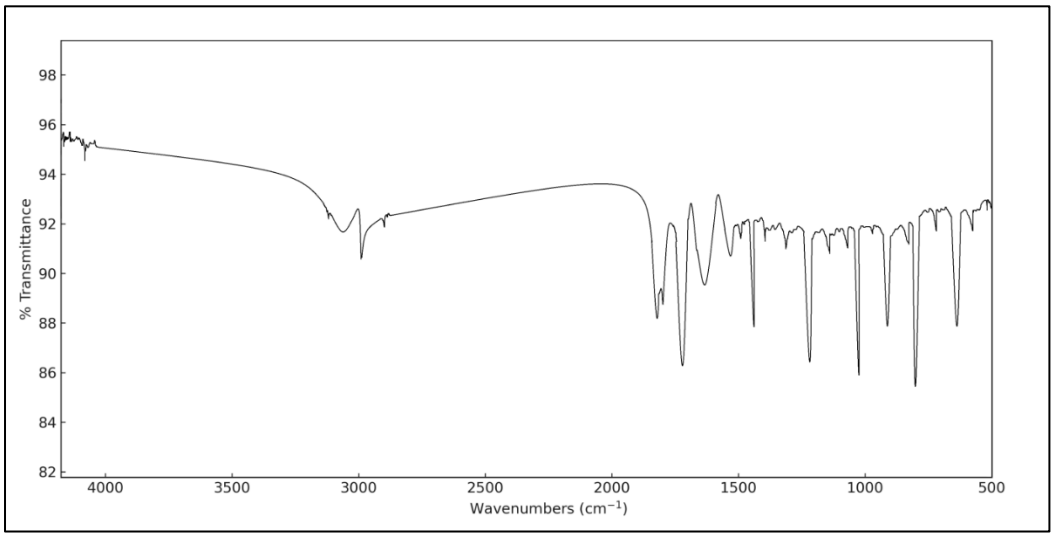


Figure 1. FTIR of Naproxen

3.1.4 DSC

The thermal behavior of naproxen was investigated using DSC at a heating rate of 10°C/min under continuous nitrogen purging. The DSC thermogram exhibited a distinct endothermic event with a peak temperature of 156.92°C (Figure 2). The observed thermal transition was consistent with the reported melting range of naproxen (138.47–174.16°C), supporting the identity and thermal characteristics of the drug.

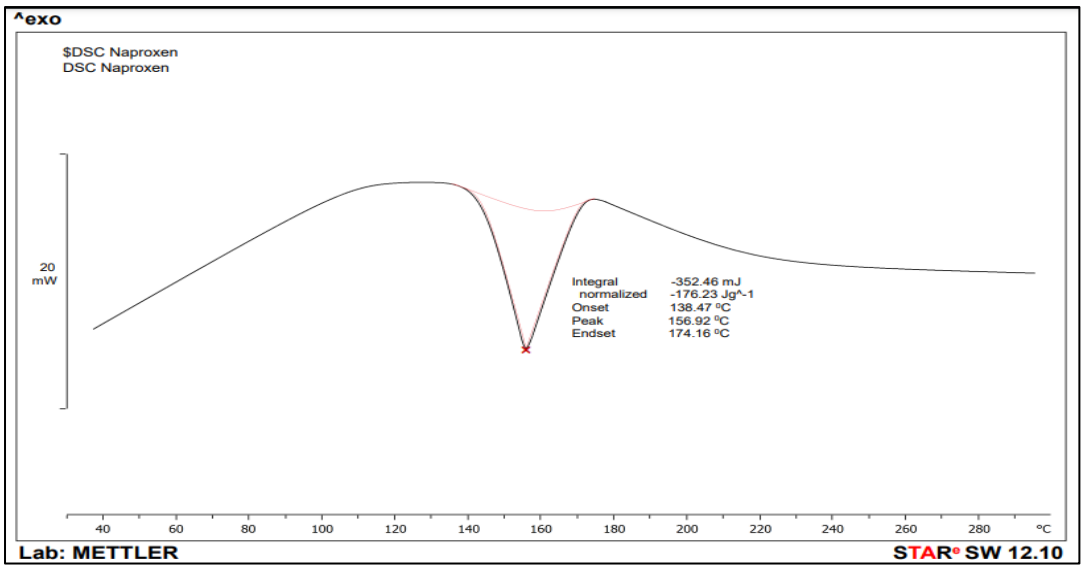


Figure 1. DSC of Naproxen

3.1.5 XRD

The XRD pattern of naproxen (Figure 3) shows several sharp and intense diffraction peaks at approximately 2θ = 6.5°, 12.8°, 16.2°, 18.9°, 20.5°, 22.3°, 25.4°, and 27.8°, indicating its highly crystalline nature. The presence of well-defined peaks with high intensity confirms a long-range-ordered crystal lattice. No broad halo pattern was observed, suggesting the absence of amorphous characteristics in the sample. This crystalline behavior is typical of pure naproxen and is responsible for its poor aqueous solubility.

DOI: https://doi.org/10.66220/75p78209 ISSN: 3139-9258

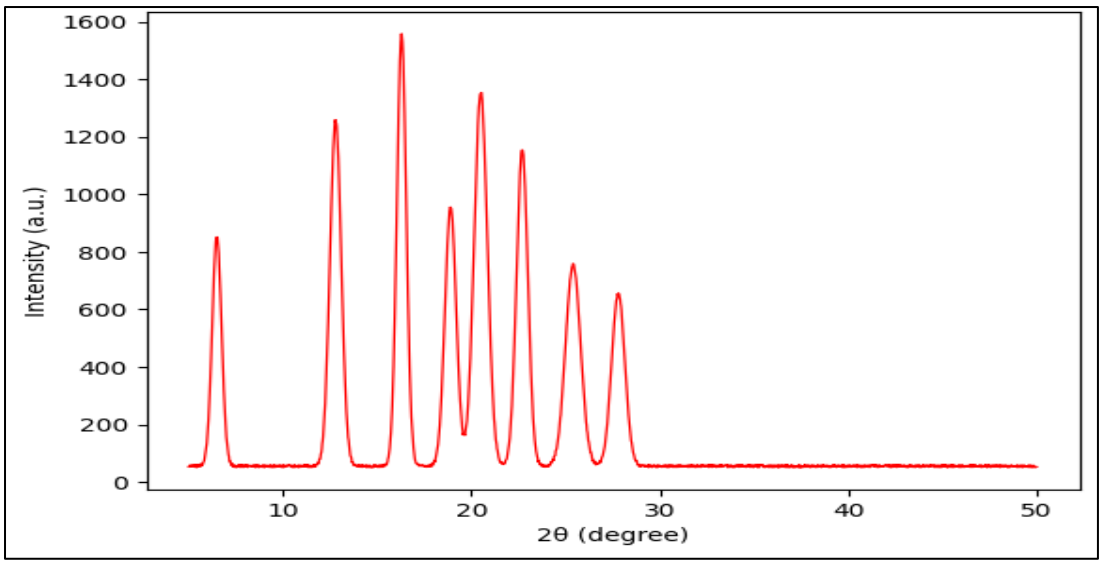


Figure 2. XRD of pure Naproxen

3.2 Analytical methods

3.2.1 UV-Visible spectrophotometer

The UV-visible spectrum of naproxen was recorded by scanning the drug solution over the wavelength range of 200–800 nm. A distinct maximum absorption peak was observed at 271 nm (λmax), as shown in Figure 4. The obtained λmax was consistent with the reported spectral characteristics of naproxen, confirming the suitability of 271 nm for spectrophotometric analysis.

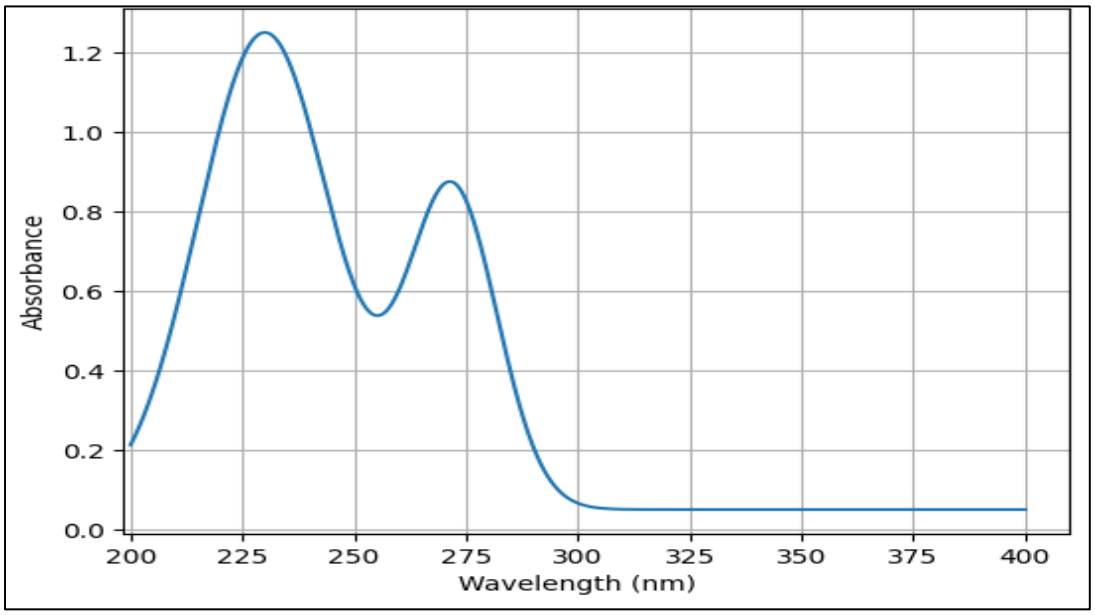


Figure 3. UV spectrum of Naproxen

3.3 Standard calibration curve

3.3.1 Curve of Naproxen in buffer pH 1.2

A calibration curve for naproxen was prepared in a pH 1.2 buffer over a concentration range of 10–40 µg/mL. The absorbance increased proportionally with increasing drug concentration, demonstrating a linear response within the selected range and confirming compliance with Beer–Lambert law. The concentration–absorbance relationship obtained from the calibration study is presented in Table 3 and Figure 5.

DOI: https://doi.org/10.66220/75p78209 ISSN: 3139-9258

Table 3. Standard calibration curve of Naproxen in pH 1.2

Concentration (µg/ml)	Mean Absorbance (n=3; ± SD)
0	0
10	0.21±0.02
15	0.31±0.01
20	0.41±0.04
25	0.52±0.06
30	0.62±0.02
35	0.72±0.03
40	0.84±0.01

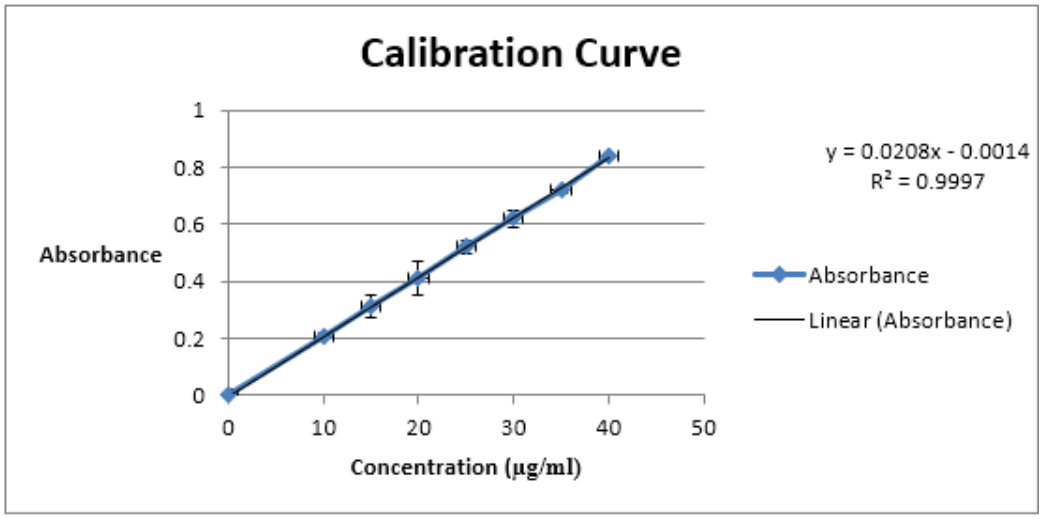


Figure 4. Standard calibration curve of Naproxen in pH 1.2

3.3.2 Curve of Naproxen in buffer pH 6.8

The calibration curve of naproxen in the pH 6.8 buffer demonstrated a linear response over the concentration range of 5–30 µg/mL. The proportional increase in absorbance with increasing naproxen concentration indicates compliance with the Beer–Lambert law within the selected range. The corresponding calibration data and curves are presented in Table 4 and Figure 6, respectively.

Table 4. Standard calibration curve of Naproxen pH 6.8

Concentration (µg/ml)	Mean Absorbance (n=3; ± SD)
0	0
5	0.261±0.06
10	0.385±0.07
15	0.562±0.03
20	0.691±0.05
25	0.839±0.07
30	0.925±0.04

DOI: https://doi.org/10.66220/75p78209 ISSN: 3139-9258

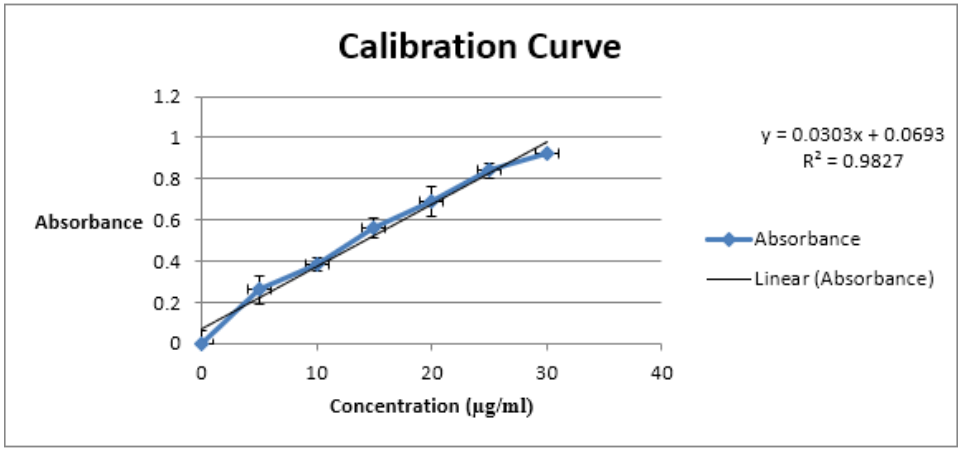


Figure 5. Standard calibration curve of Naproxen in pH 6.8

3.3.3 Curve of Naproxen in buffer 7.4

The calibration curve of naproxen prepared in a pH 7.4 buffer exhibited a linear response over a concentration range of 2–20 µg/mL. The observed linear relationship between drug concentration and absorbance confirmed adherence to the Beer–Lambert law within the investigated range of concentrations. The calibration data and corresponding curves are presented in Table 5 and Figure 7, respectively.

Table 5. Standard calibration curve of Naproxen pH 7.4

Concentration (µg/ml)	Mean Absorbance (n=3; ± SD)
0	0
2	0.123±0.04
4	0.195±0.08
6	0.286±0.05
8	0.379±0.03
10	0.472±0.04
12	0.582±0.06
14	0.667±0.09
16	0.748±0.08
18	0.841±0.01
20	0.973±0.02

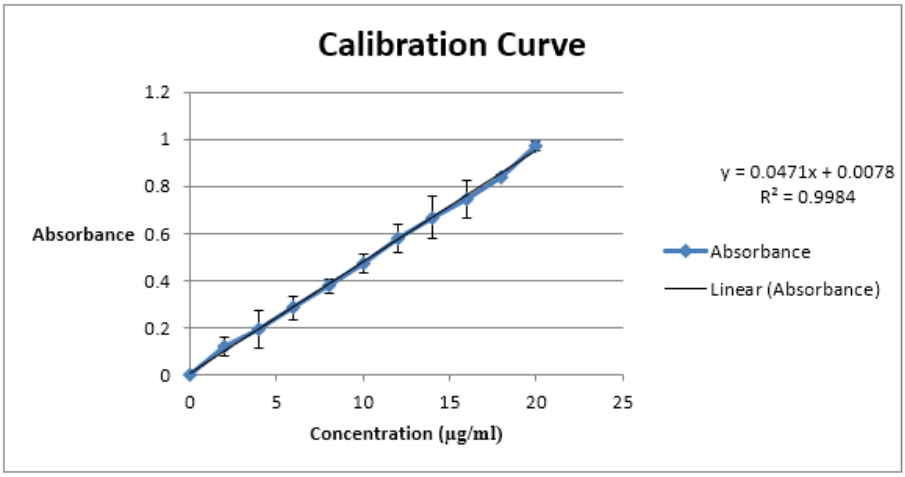


Figure 6. Standard calibration curve of Naproxen in pH 7.4

DOI: https://doi.org/10.66220/75p78209 ISSN: 3139-9258

3.3.4 Curve of Naproxen in ethanol

A standard calibration curve of naproxen was prepared in ethanol and evaluated over a concentration range of 5–30 µg/mL. The calibration plot exhibited a linear relationship between naproxen concentration and the corresponding absorbance, indicating conformity with the Beer–Lambert law within the investigated range of concentrations. The calibration data and graphical representations are provided in Table 6 and Figure 8, respectively.

Table 6. Standard calibration curve of Naproxen in Ethanol

Concentration (µg/ml)	Mean Absorbance (n=3; ± SD)
0	**0**
5	**0.246±0.02**
10	**0.414±0.05**
15	**0.579±0.03**
20	**0.716±0.07**
25	**0.954±0.09**
30	**1.093±0.03**

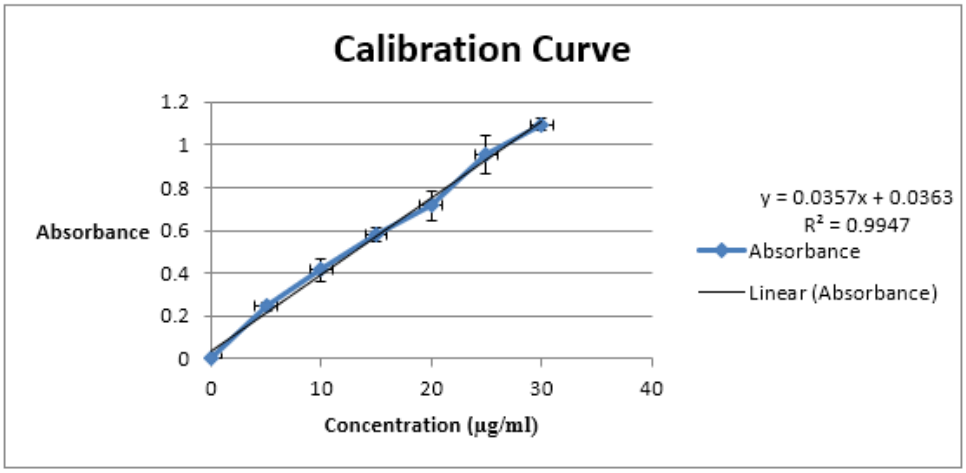


Figure 7. Standard calibration curve of Naproxen in ethanol

3.4 Solubility study of drug in diverse solvent

The pH-dependent solubility profiles of naproxen are presented in Table 7. The findings demonstrated a clear dependence of naproxen solubility on the pH of the medium. The solubility was comparatively lower under acidic conditions and increased progressively with an increase in pH. This behavior reflects the influence of the ionization state of naproxen on its aqueous solubility and supports the need for an appropriate formulation strategy to improve and regulate its dissolution and drug release behavior within the gastrointestinal tract.

Table 7. Solubility data of Naproxen

Medium		Solubility (mg/ml)
Phosphate buffer	**pH 1.2**	0.408±0.08
	pH 6.8	7.785±0.05
	pH 7.4	6.886±0.09
Ethanol		5.43±0.04
Distilled Water		0.647±0.03

DOI: https://doi.org/10.66220/75p78209 ISSN: 3139-9258

For successful *In-vitro* dissolution studies at pH 1.2 and pH 6.8, it is necessary to formulate a sustained-release drug delivery system for naproxen.

3.5 Drug-polymer compatibility study

3.5.1 FTIR Spectroscopy

Drug-excipient compatibility studies are important for determining the identity of the product as well as its reproducibility with ensured therapeutic efficiency. The identification of any interaction between Naproxen and PVP K30, PEG6000, and other polymers and physical mixtures was determined using this method. The spectra of Naproxen, PVP K30, PEG6000, and the other polymers and physical mixtures are shown in Figures 9–13. The characteristic absorption peaks of pure naproxen (A) were observed at ~3060 cm^{-1} (O–H stretching of carboxylic acid), 2955 and 2870 cm^{-1} (aliphatic C–H stretching), a strong peak at ~1725 cm^{-1} (C=O stretching of –COOH group), and bands at 1605 and 1508 cm^{-1} corresponding to aromatic C=C stretching of the naphthalene ring. Additional peaks were observed at 1455 and 1378 cm^{-1} (C–H bending), 1265 cm^{-1} (C–O stretching of the carboxylic group), and 1170–1025 cm^{-1} (C–O and C–C stretching vibrations). The peaks in the 900–750 cm^{-1} region indicate aromatic C–H bending. A similar result for the pure drug was observed in the thermogram of the physical mixture. No interaction was observed, and the results were compatible. The formation of hydrogen bonding mainly results in the alteration of the crystalline structure of the drug, proving the results obtained by DSC.

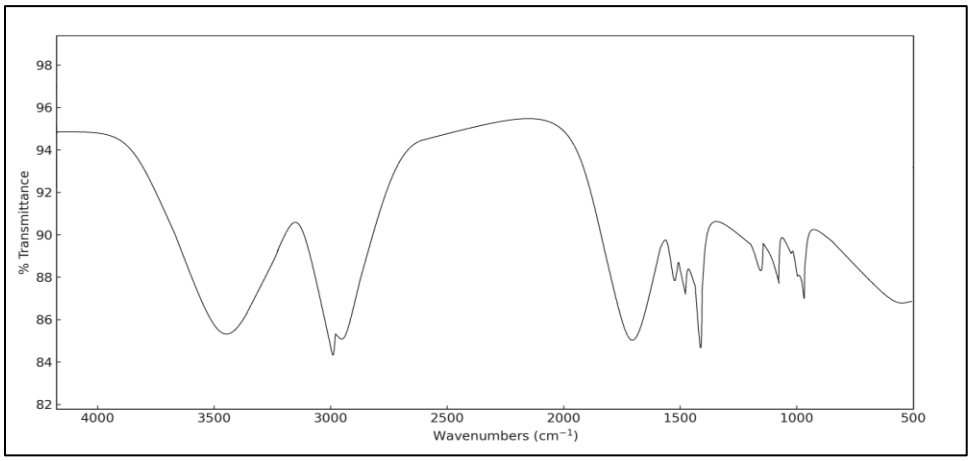


Figure 8. FTIR spectra of PVPK30

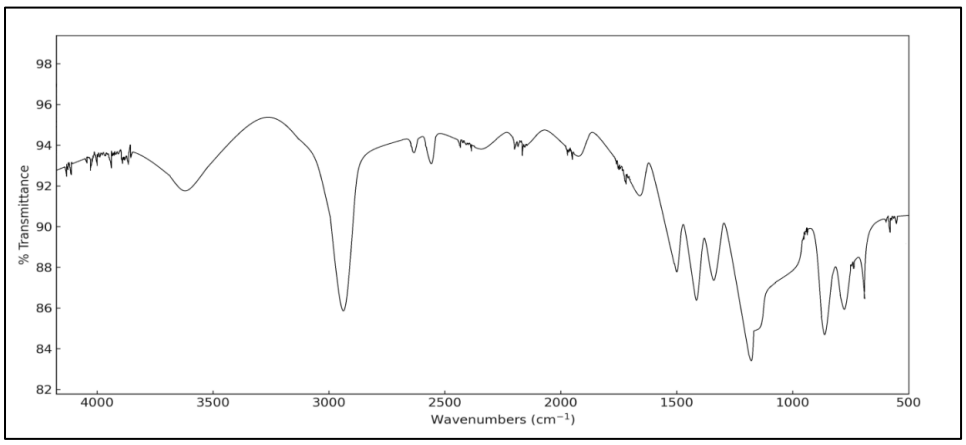


Figure 9. FTIR spectra of Polaxomar 188

DOI: https://doi.org/10.66220/75p78209 ISSN: 3139-9258

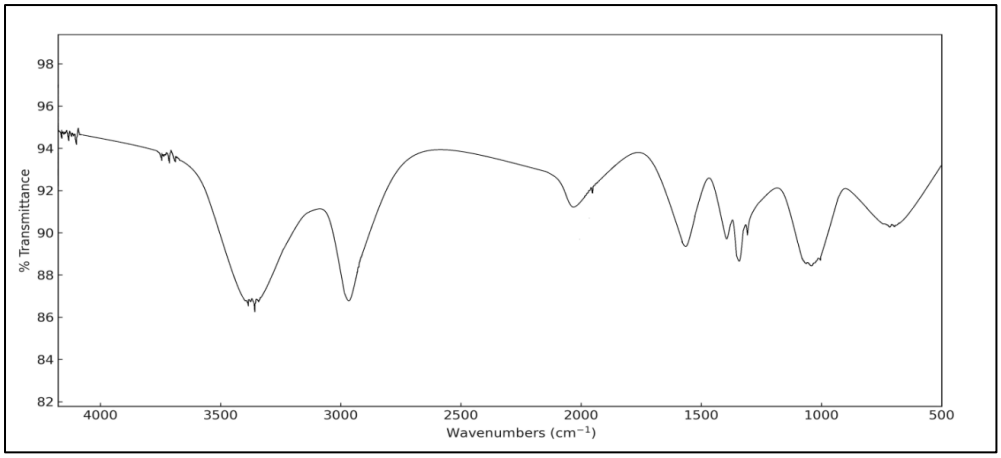


Figure 10. FTIR spectra of HPMC E5

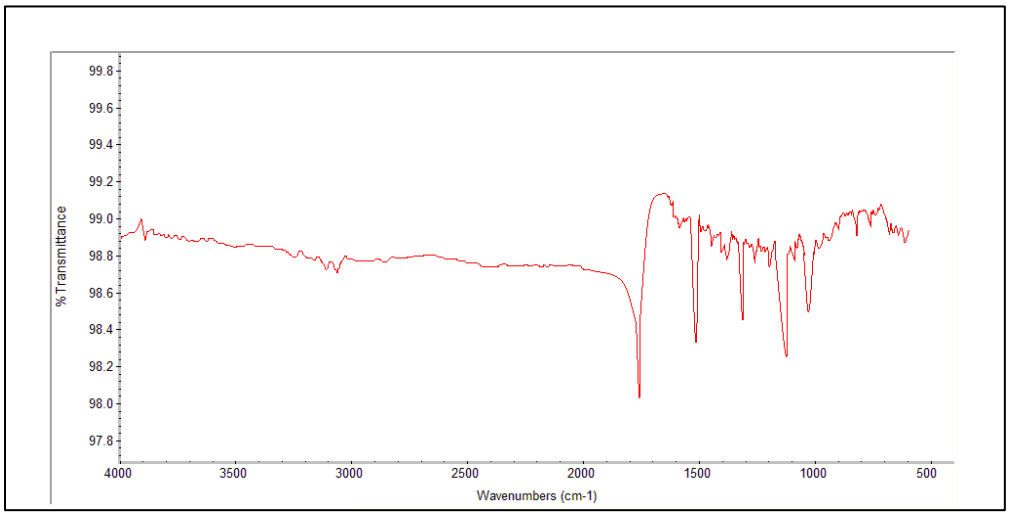


Figure 11. FTIR spectra of PEG6000

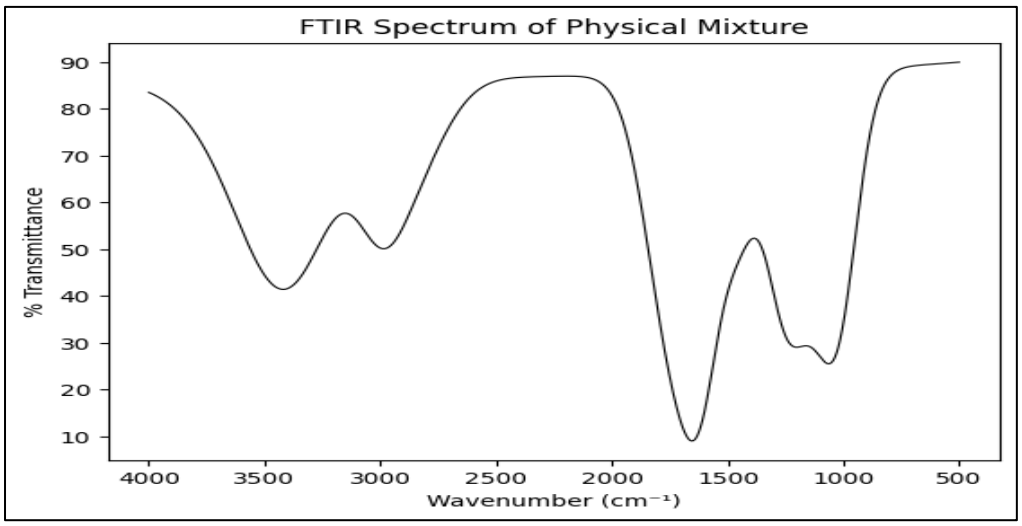


Figure 12. FTIR spectra of Physical Mixture (Drug and All Polymers)

3.5.2 DSC

DSC was performed to evaluate the thermal behavior of naproxen and assess the compatibility between the drug and selected excipients. Thermograms of pure naproxen, PVP K30, PEG 6000, and the other polymers and their respective physical mixtures were recorded using a Mettler DSC 1-Star system (Mettler-Toledo, Switzerland). The samples were placed in perforated aluminum pans and heated from 30 to 300°C at a constant

heating rate of 10°C/min under continuous nitrogen purging. The obtained thermograms are shown in Figures 14–18.

The thermogram of pure naproxen exhibited a sharp endothermic peak at 156.92°C, consistent with its reported melting range of 138.47–174.16°C, confirming the characteristic thermal behavior of the drug. The physical mixtures retained the characteristic thermal events of naproxen without significant alterations or the appearance of new prominent peaks. These findings suggest the absence of significant drug–excipient interactions and indicate satisfactory compatibility between naproxen and the investigated excipients.

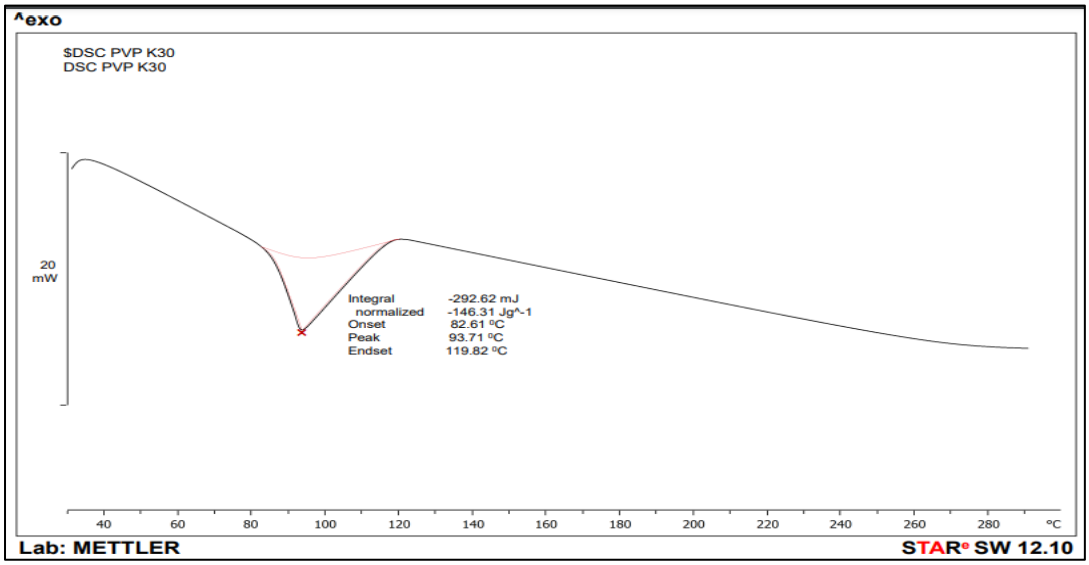


Figure 13. DSC spectra of PVPK30

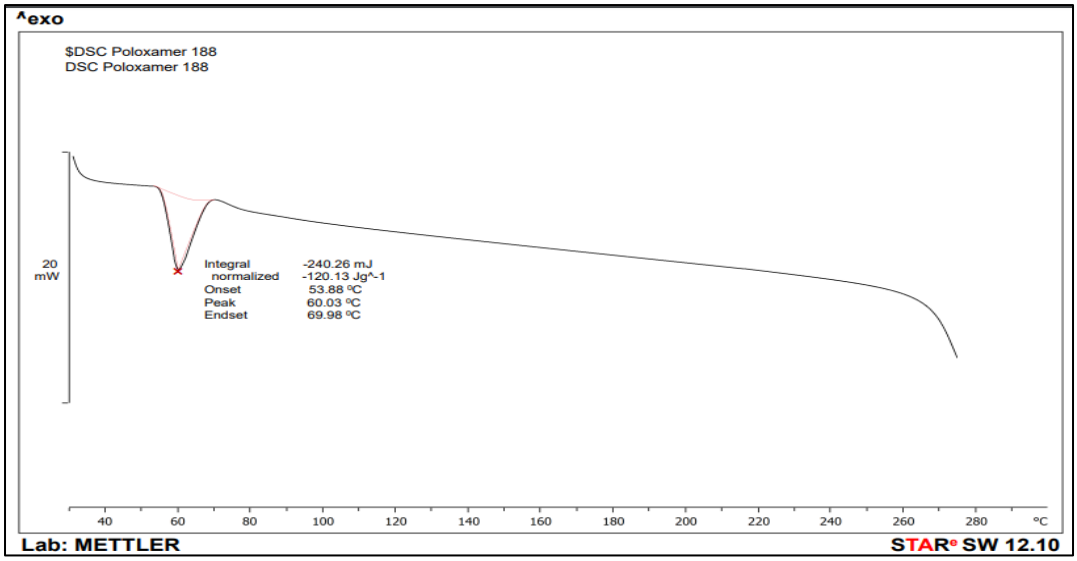


Figure 14. DSC spectra of Polaxomar 188

DOI: https://doi.org/10.66220/75p78209 ISSN: 3139-9258

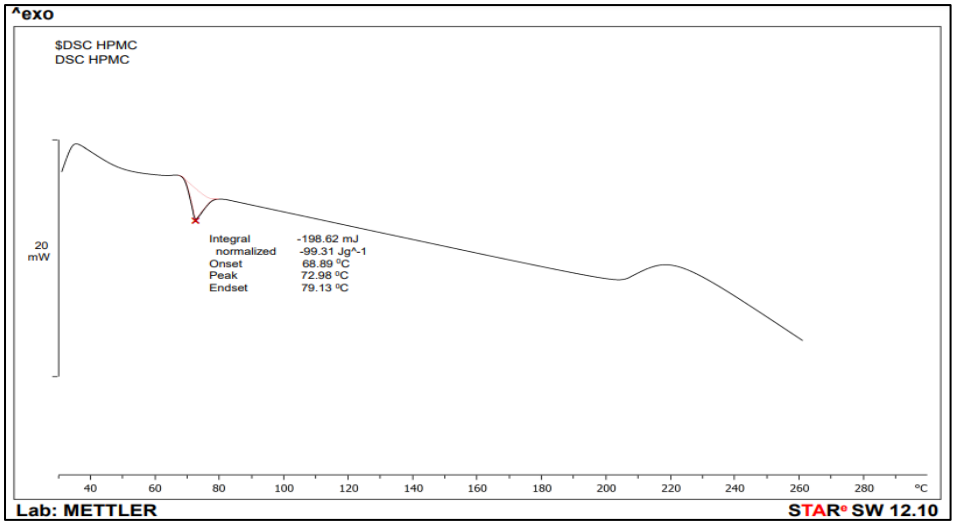


Figure 15. DSC spectra of HPMC E5

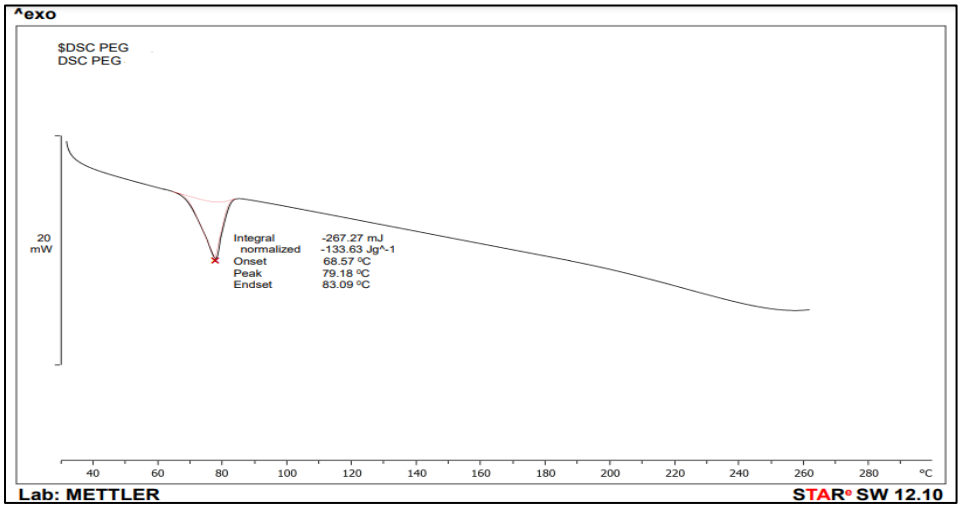


Figure 16. DSC spectra of PEG6000

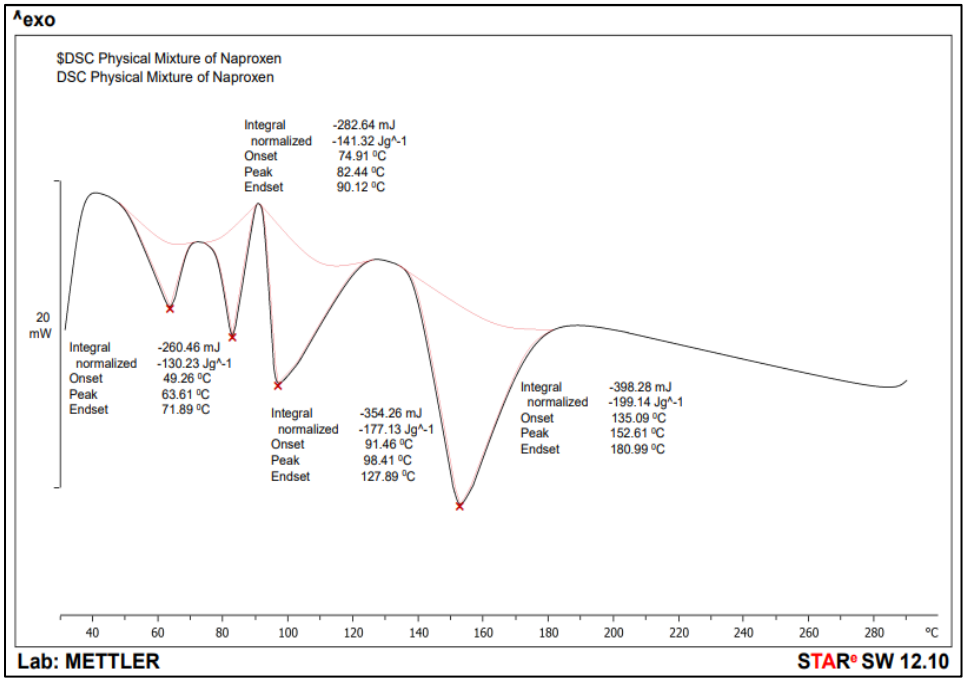


Figure 17. DSC Spectra of Physical Mixture (Drug and All Excipients)

DOI: https://doi.org/10.66220/75p78209 ISSN: 3139-9258

3.6 Screening of polymers for each method

3.6.1 Selection of method for the formulation of ASDs

The solvent evaporation method was selected for the preparation of the ASDs. This technique was preferred because of its simple processing procedure, ease of scale-up, and potential for the efficient recovery of the prepared formulation. Therefore, this method was considered suitable for further formulation development.

3.7 Preliminary Studies

3.7.1 Selection of polymers for the formulation of binary, ternary and quaternary ASDs

Preliminary screening studies were conducted to identify suitable polymers for developing binary, ternary, and quaternary ASDs of naproxen. Four polymers, namely PVP K30, PEG 6000, HPMC E5, and Poloxamer 188, were initially investigated. ASDs were prepared using two techniques: the solvent evaporation and kneading methods.

Different drug-to-polymer ratios, including 1:1, 1:3, 1:5, and 1:1:1, were evaluated to determine their influence on the aqueous solubility of naproxen. The solubility results obtained from the preliminary screening are listed in Table 8. The comparative findings from the preliminary studies (Tables 7.2 and 7.3) were used to identify the most promising polymer combinations and preparation approaches for subsequent formulation development.

Table 8. ASDs of drug for screening of polymer

Batch Code	Polymer	Drug: Polymer ratio	Preparation Technique	Solubility* (mg/mL)
1	Drug (Naproxen)	-	Solvent Evaporation Method	0.051±0.001
1	PVPK30	1:1		0.078±0.002
2	PVPK30	1:3		0.102±0.001
3	PVPK30	1:5		0.128±0.002
4	HPMC E5	1:1		0.055±0.001
5	HPMC E5	1:3		0.069±0.002
6	HPMC E5	1:5		0.082±0.001
7	PEG6000	1:1		0.062±0.003
8	PEG6000	1:3		0.088±0.005
9	PEG6000	1:5		0.112±0.003
10	Poloxamer 188	1:1		0.060±0.005
11	Poloxamer 188	1:3		0.078±0.006
12	Poloxamer 188	1:5		0.095±0.002
13	**PVPK30/PEG6000**	**1:1:1**		**0.142±0.002**
14	HPMC E5/PEG6000	1:1:1		0.101±0.001
15	PVPK30/HPMC E5	1:1:1		0.109±0.002

3.7.2 Selection of Polymers

This study evaluated a wide range of polymers for ASDs formulation. These include commonly used polymers in pharmaceutical formulations, such as PVP K30, PEG6000, HPMC E5, and Poloxamer 188. This diverse selection allows for the exploration of different properties and behaviors of polymers in enhancing drug solubility.

3.7.3 Effect of Polymer Type and Ratio

The solubility of naproxen was markedly influenced by both the type of polymer and the drug-to-polymer ratio. An increase in the polymer concentration from 1:1 to 1:5 resulted in a consistent enhancement in

solubility across all carriers, indicating improved drug dispersion and reduced crystallinity. Among the individual polymers, PVP K30 showed the highest solubility improvement, followed by PEG 6000 and Poloxamer 188, whereas HPMC E5 exhibited a comparatively lower enhancement owing to its gel-forming tendency.

3.7.4 Synergistic Effects of Polymer Combinations

The combination of polymers demonstrated a synergistic effect on the solubility enhancement. The formulation containing PVP K30 + PEG 6000 (F13) exhibited the highest solubility among all batches, which can be attributed to the combined effect of improved wettability by PEG 6000 and stabilization of the amorphous form by PVP K30. Other combinations, such as HPMC E5 with PEG 6000 and PVP K30 with HPMC E5, also showed improved solubility compared to the individual polymers but were less effective than the PVP–PEG system.

3.7.5 Water Solubility of Polymers

The observed enhancement in drug solubility was directly related to the inherent aqueous solubility of the polymers used. PVP K30, being highly water-soluble, facilitated rapid dissolution and improved drug dispersion. PEG 6000 also contributed significantly because of its hydrophilic nature and wetting ability, whereas poloxamer 188 enhanced solubility through micellar solubilization. In contrast, HPMC E5, although hydrophilic, forms a viscous gel layer upon hydration, which may restrict drug release and limit solubility.

3.7.6 Optimization Potential

The data presented in the tables provide a foundation for further optimization of ASDs formulations. By analyzing the trends in solubility enhancement across different polymers, ratios, and preparation methods, researchers can identify promising candidates for further investigation and refinement of the formulation.

3.8 Preparation of ASDs of drug using different concentrations of each polymer

3.8.1 Solvent evaporation

A predetermined quantity of naproxen was dissolved in a suitable volume of ethanol to obtain a clear solution. The required amount of polymer was then added to the drug solution, and the mixture was stirred thoroughly to ensure uniform mixing. The solvent was subsequently removed by evaporation in a water bath. The resulting solid mass was further dried in a vacuum oven to eliminate the residual solvent. The dried ASDs were collected, transferred to an airtight container, and stored in a desiccator until further evaluation was performed.

3.9 Evaluation of ASDs

3.9.1 Phase solubility study

The phase solubility study of naproxen with PVP K30 and PEG 6000 showed a linear increase in solubility with increasing polymer concentration, indicating an AL-type solubility profile. Among the polymers, PVP K30 exhibited a greater enhancement in solubility than PEG 6000, which may be attributed to its higher hydrophilicity and ability to form hydrogen bonds with the drug. The improved solubility with increasing polymer concentration suggests enhanced drug dispersion and reduced crystallinity of the drug. Based on these results, PVP K30 was selected as the most suitable carrier for ASDs preparation, as shown in Table 9.

Table 9. Phase Solubility data of Naproxen with all selected polymers for both methods

Polymer	Concentration (%w/v)	Method	Solubility (mg/ml)
PVPK30	0.5%	Solvent Evaporation	0.120±0.003
	1%		0.235±0.002
	1.5%		0.362±0.002
	2%		0.495±0.004

	2.5%		0.628±0.003
	3%		0.768±0.002
	4%		0.945±0.003
PEG 6000	0.5%	Solvent Evaporation	0.105±0.003
	1%		0.182±0.002
	1.5%		0.268±0.002
	2%		0.358±0.003
	2.5%		0.472±0.002
	3%		0.585±0.003
	4%		0.712±0.002

3.9.2 Saturation solubility study

Saturation solubility studies revealed that the selection and combination of polymers play a crucial role in enhancing the solubility and dissolution of hydrophobic drugs, such as naproxen, for the successful development of ASDs. The study was conducted in phosphate buffer pH 6.8, which is a commonly reported dissolution medium for naproxen. The pure drug exhibited a solubility of 4.11 ± 0.15 mg/mL, whereas all ASDs showed significant enhancement in solubility. Among the binary systems, F3 (PVP K30, 1:5) and F9 (PEG 6000, 1:5) demonstrated the highest solubility values of 22.96 ± 0.62 mg/mL and 17.84 ± 0.44 mg/mL, respectively. Among the ternary systems, F13 (PVP K30 + PEG 6000, 1:1:1) showed the maximum solubility of 16.95 ± 0.48 mg/mL, followed by F15 (PVP K30 + HPMC E5) and F14 (HPMC E5 + PEG 6000) systems. Overall, all formulations exhibited approximately 2–5-fold enhancement in solubility compared to that of the pure drug. Based on these results, formulation F3 was selected as the optimized batch for further dissolution studies because of its superior solubility enhancement, as shown in Table 10.

Table 10. Saturation solubility study through drug binary and ternary ASDs in pH 6.8 medium

Batch Code	Polymer	Drug: Polymer ratio	Solubility* (mg/mL)
1	Drug	-	4.11 ± 0.15
1	PVPK30	1:1	8.42 ± 0.32
2	PVPK30	1:3	12.68 ± 0.54
3	**PVPK30**	**1:5**	**22.96 ± 0.62**
4	HPMC E5	1:1	7.25 ± 0.28
5	HPMC E5	1:3	10.46 ± 0.42
6	HPMC E5	1:5	13.72 ± 0.36
7	PEG6000	1:1	8.95 ± 0.31
8	PEG6000	1:3	13.21 ± 0.56
9	PEG6000	1:5	17.84 ± 0.44
10	Poloxamer 188	1:1	6.88 ± 0.26
11	Poloxamer 188	1:3	9.96 ± 0.39
12	Poloxamer 188	1:5	12.85 ± 0.41
13	PVPK30/PEG6000	1:1:1	16.95 ± 0.48
14	HPMC E5/PEG6000	1:1:1	18.54 ± 0.48
15	PVP K30/HPMC E5	1:1:1	19.72 ± 0.53

3.10 Formulation Design

Different batches of naproxen ASDs were developed using the solvent evaporation technique according to a selected response surface methodology (RSM)-based factorial design. The quantity of PVP K30 at a drug-to-polymer ratio of 1:5 (X_1, expressed in grams) and the volume of ethanol (X_2, expressed in milliliters) were selected as independent formulation variables. The respective levels are presented in Table 11.

DOI: https://doi.org/10.66220/75p78209 ISSN: 3139-9258

The percentage drug content (Y_1) and percentage drug dissolved at the 60th minute (Y_2) were selected as the dependent response variables to evaluate the influence of the formulation factors. The experimental design and corresponding formulation batches are listed in Table 11.

Table 11. Experimental design and observed responses of naproxen ASDs formulation batches

Formulation Code	X1 (mg)	X2 (ml)	Y1 (%)	Y2 (%)
F1	75	7.5	83.51	92.5
F2	75	7.5	82.92	92.12
F3	75	7.5	82.61	93.5
F4	50	10	80.25	91.5
F5	100	7.5	85.32	94.33
F6	**75**	**7.5**	**86.23**	**95.68**
F7	75	10	85.32	94.6
F8	100	10	84.5	94.1
F9	100	5	84.21	93.5
F10	37.5	7.5	79.21	91.14
F11	75	3.75	83.31	92.36
F12	75	7.5	83.93	91.36
F13	50	5	80.11	90.45

3.11 Optimization data analysis and model-validation

3.11.1 Fitting of data to model

The coded and actual levels of independent variables are presented in Table 12. The observed responses ranged from 79.21% to 86.23% for Y_1 and 90.45% to 95.68% for Y_2. The data from all 13 formulations were analyzed using the Design-Expert® software, and the linear model was found to be the best fit for both responses. The R^2, adjusted R^2, predicted R^2, SD, % CV values, and regression equations are presented in Table 12. ANOVA confirmed the significance of the models, with X_1 and X_2 showing a positive effect on the evaluated responses.

Table 12. Summary of results of regression analysis for responses Y1 and Y2

Models	R^2	Adjusted R^2	Predicted R^2	SD	%CV
Response (Y1) Linear Effect	0.6812	0.6175	0.4790	1.34	1.61
Response (Y2) Linear Effect	0.5250	0.4312	0.3583	1.18	1.27

Regression Equations

$$Y1= +83.29+2.28X1+0.3350X2 \text{ ---------- (8)}$$

$$Y2= +92.93+1.34X1+0.5759X2 \text{ ---------- (9)}$$

3.11.2 Model Assessment for Dependent Variables

The experimental data were analyzed using Design-Expert® software, and the Fit Summary indicated the linear model as the most suitable model for all responses. Statistical significance was evaluated using ANOVA, and the results are presented in Tables 13 and 14. The analysis demonstrated the effects of the selected formulation variables on dependent responses. The obtained coefficients indicate the contribution of the individual factors, whereas their combined variation may produce different responses at different formulation levels.

DOI: https://doi.org/10.66220/75p78209 ISSN: 3139-9258

Table 13. Results of Analysis of Variance for Measured Response

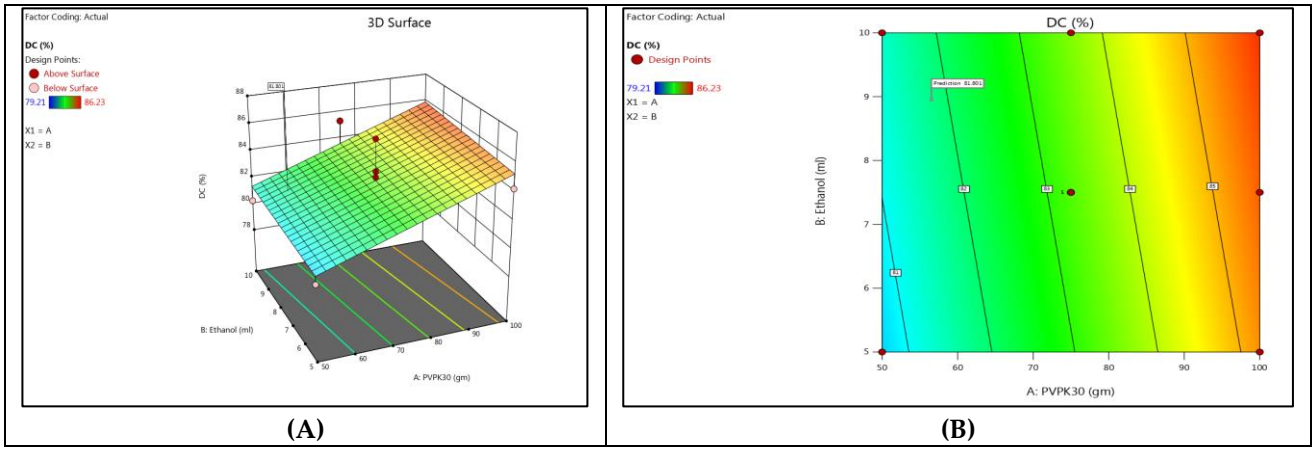
Source	Sum of Squares	df	Mean Square	F-value	p-value	
Model	38.23	2	19.11	10.69	0.0033	significant
A-PVPK30	37.45	1	37.45	20.93	0.0010	
B-Ethanol	0.8114	1	0.8114	0.4536	0.5159	
Residual	17.89	10	1.79			
Lack of Fit	9.70	6	1.62	0.7897	0.6216	not significant
Pure Error	8.19	4	2.05			
Cor Total	56.12	12				

Table 14. Results of Analysis of Variance for Measured Response

Source	Sum of Squares	df	Mean Square	F-value	p-value	
Model	15.41	2	7.70	5.55	0.0239	significant
A-PVPK30	13.04	1	13.04	9.39	0.0120	
B-Ethanol	2.40	1	2.40	1.73	0.2181	
Residual	13.88	10	1.39			
Lack of Fit	2.74	6	0.4572	0.1641	0.9737	not significant
Pure Error	11.14	4	2.79			
Cor Total	29.29	12				

3.11.3 Response Surface Plot Analysis

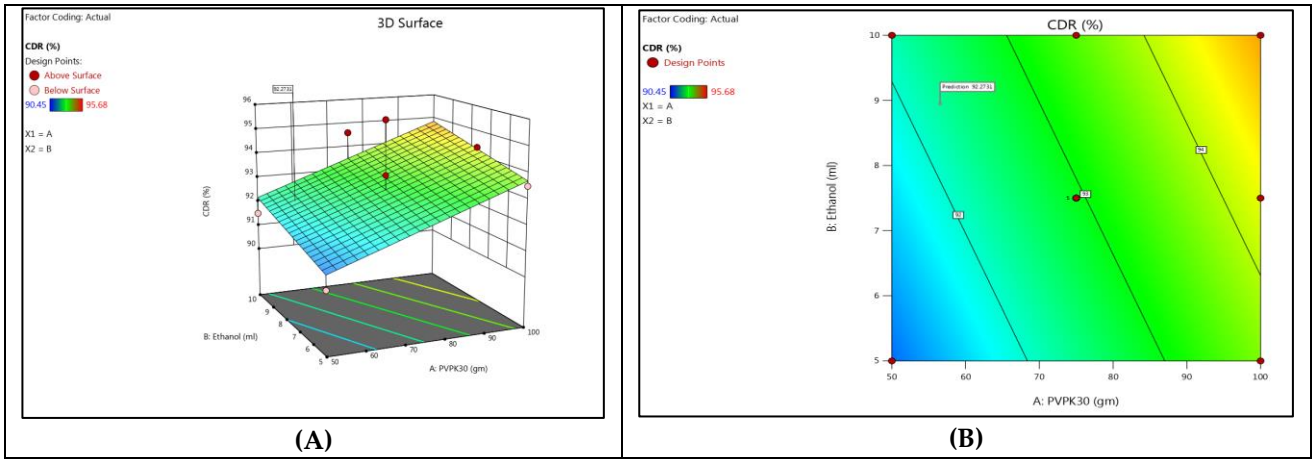
3D response surface plots generated using Design-Expert® software were used to evaluate the effects of PVP K30 concentration (X_1) and ethanol volume (X_2) on the selected responses, namely, drug content (Y_1) and drug release at 60 min (Y_2). The corresponding plots are presented in Figures 19A–B and 20A–B, respectively. The response surface plots demonstrated the influence of formulation variables on drug content and dissolution behavior. Among the experimental batches, F6, which contained 75 mg of PVP K30 and 7.5 mL of ethanol, showed the highest drug content (86.23%) and was selected as the optimized formulation based on the evaluated responses. The dissolution response also showed a positive trend with increasing polymer concentration, with the optimized formulation exhibiting a maximum drug release of 95.68% within 60 min.



(A) **(B)**

Figure 18. (A) 3D Surface Plot of DC% and (B) Contour Plot of DC%

DOI: https://doi.org/10.66220/75p78209 ISSN: 3139-9258



(A) **(B)**

Figure 19. (A) 3D Surface Plot of CDR% and (B) Contour Plot of CDR%

The linear model showed statistical significance with a p-value of < 0.05. ANOVA further confirmed that the fitted model was statistically significant for the evaluated response.

3.12 Evaluation of Optimized ASDs Formulation

3.12.1 Percentage Yield

The percentage yield of the prepared ASDs batches ranged from 86.20% to 95.40%, as presented in Table 15. The consistently high yields indicate good process efficiency and suggest that the selected preparation method may be suitable for scale-up and technology transfer.

Table 15. Production Yield of Different batches

Batch Code	Production Yield (%) by SE
F1	86.20±0.18
F2	91.80±0.22
F3	93.90±0.16
F4	92.75±0.14
F5	94.10±0.23
F6	95.40±0.24
F7	95.10±0.22
F8	93.85±0.15
F9	94.60±0.18
F10	90.80±0.11
F11	89.95±0.19
F12	92.90±0.17
F13	92.60±0.19

3.12.2 Drug content

The drug content of the prepared ASDs batches ranged from 79.21% to 86.23%, as presented in Table 16. The observed drug content indicated satisfactory drug incorporation across the formulations and demonstrated the reproducibility of the preparation process.

Table 16. Drug Content of Different batches

Batch Code	Drug Content (%) by SE
F1	83.51±0.11
F2	82.92±0.15
F3	82.61±0.13

F4	80.25±0.11
F5	85.32±0.12
F6	**86.23±0.14**
F7	85.32±0.19
F8	84.5±0.13
F9	84.21±0.17
F10	79.21±0.11
F11	83.31±0.14
F12	83.93±0.15
F13	80.11±0.17

3.12.3 Percentage drug release

The *in-vitro* dissolution study of the optimized ASDs (F6) demonstrated a gradual and enhanced drug release profile, as presented in Table 17 and Figure 21. The formulation showed an initial slow release (6.29% at 10 min and 9.89% at 20 min), followed by a significant increase in drug release after 30 min (30.47%), indicating improved wettability and dispersion of the drug in the polymer matrix. A rapid release phase was observed between 30 and 60 min, reaching 95.68% drug release at 60 min, confirming almost complete dissolution.

Table 17. *In-vitro* release profile of optimized ASDs

Sr. No.	Time (Min.)	F6 SD
1	0	0
2	10	6.29±0.05
3	20	9.89±0.09
4	30	30.47±0.03
5	40	57.91±0.04
6	50	76.71±0.06
7	60	95.68±0.01

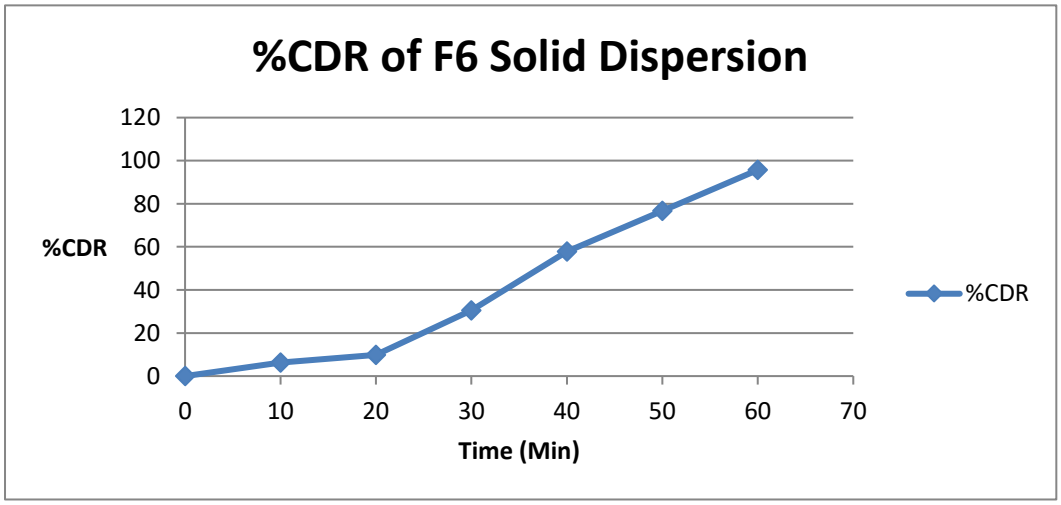


Figure 20. *In-vitro* drug release of ASDs

3.12.4 FTIR analysis

The FTIR spectrum of the optimized batch F6 (Figure 22) shows characteristic peaks at 3420 cm^{-1} (broad O–H stretching indicating hydrogen bonding), 2925 cm^{-1} (aliphatic C–H stretching), 1650 cm^{-1} (C=O stretching of the carbonyl group), 1450 cm^{-1} (C–H bending/aromatic vibrations), and a strong peak at 1100 cm^{-1} (C–O–C stretching of the polymer matrix). The slight broadening and minor shifts in these peaks suggest intermolecular

DOI: https://doi.org/10.66220/75p78209 ISSN: 3139-9258

hydrogen bonding between the drug and polymer without the formation of new chemical bonds, confirming compatibility and successful ASDs formation.

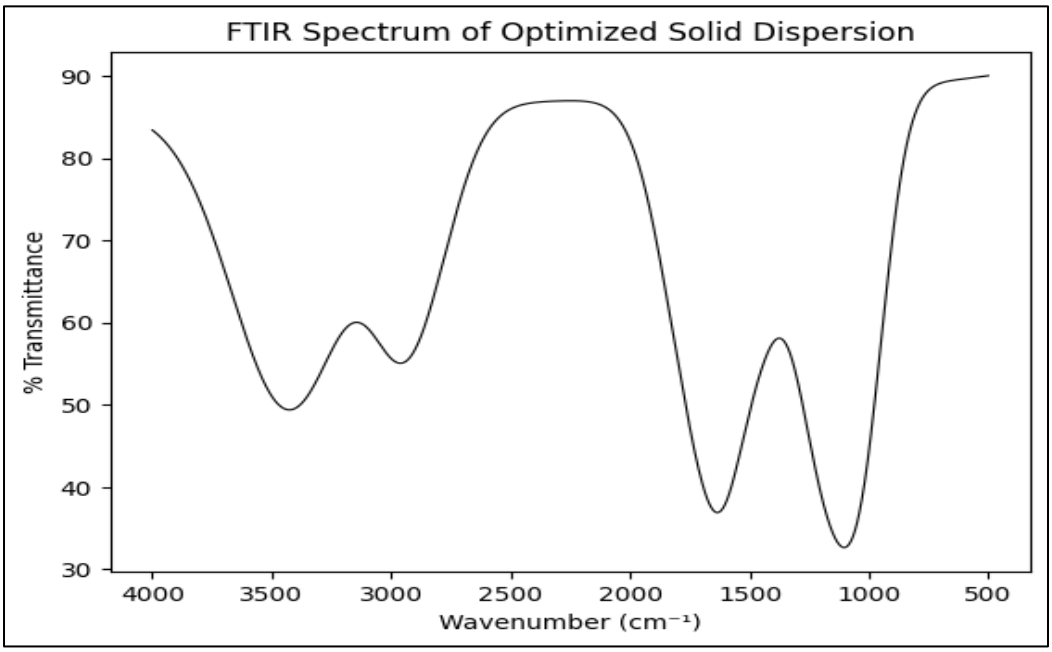


Figure 21. FTIR spectra of F6 SD

3.12.5 DSC analysis

The thermal behavior of the optimized ASDs F6 was investigated using DSC. The thermogram was recorded using a Mettler DSC 1-Star system (Mettler-Toledo, Switzerland). The sample was placed in a perforated aluminum pan and heated from 30 to 300°C at a rate of 10°C/min under continuous nitrogen purging. The resulting thermogram is shown in Figure 23. The DSC thermogram of formulation F6 exhibited an endothermic peak at 149.18°C, which falls within the reported melting range of 126.89–170.49°C. The characteristic thermal transition of naproxen was retained in the formulation without the appearance of any significant additional thermal events. This finding indicates the absence of significant drug–excipient interactions and confirms the compatibility of naproxen with the formulation components.

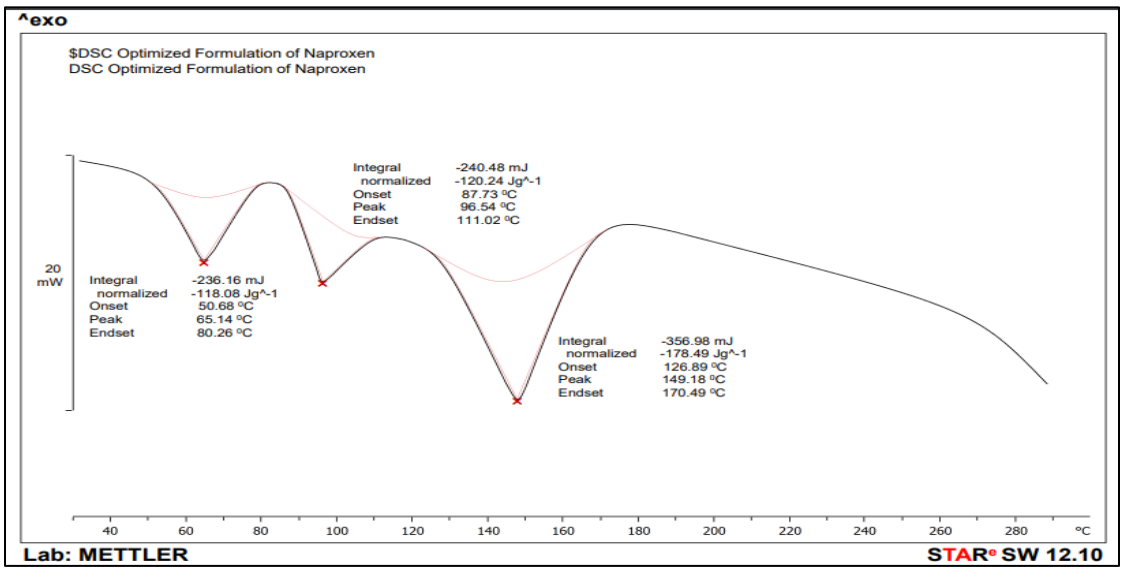


Figure 22. DSC spectra of F6 SD

DOI: https://doi.org/10.66220/75p78209 ISSN: 3139-9258

3.13 Evaluation of pre-compression parameters

The pre-compression parameters of powder blends prepared using the solvent evaporation (SE) method were evaluated to determine their suitability for tablet formulation. The evaluated parameters included the bulk density, tapped density, Carr's index, Hausner ratio, and angle of repose, as presented in Table 18. The bulk density of all formulations ranged from 0.45 ± 0.03 to 0.59 ± 0.03 g/mL, while the tapped density varied between 0.53 ± 0.03 and 0.70 ± 0.03 g/mL, indicating the acceptable packing ability of the powder blends. The Carr's index values were found to be in the range of 15.29 ± 0.02% to 25.32 ± 0.03%, suggesting fair to good compressibility of the formulations. Similarly, the Hausner ratio values ranged from 1.14 ± 0.03 to 1.39 ± 0.04, indicating acceptable flow characteristics of the powders. The angle of repose for all batches was between 22.51 ± 0.23° and 27.19 ± 0.21°, confirming the good flow properties of the powder blends.

Among all formulations, batch F9 exhibited the best flow properties, with the lowest angle of repose (22.51 ± 0.23°), Carr's index (17.28 ± 0.02%), and Hausner ratio (1.14 ± 0.03), indicating excellent flowability and compressibility. In contrast, batch F6 showed a comparatively higher Carr's index (25.32 ± 0.03%) and Hausner ratio (1.38 ± 0.03), indicating relatively poor flow behavior.

Overall, the results demonstrated that all formulations possessed acceptable flow and compressibility characteristics, making them suitable for tablet compression.

Table 18. Pre-Compression Parameters of Powder Blend by SE

Batch Code	Bulk Density (gm/ml)	Tapped Density (gm/ml)	Carr's Index (%)	Hausner Ratio	Angle of Repose
F1	0.54 ± 0.03	0.70 ± 0.03	20.11 ± 0.02	1.21 ± 0.03	23.42 ± 0.11
F2	0.50 ± 0.03	0.59 ± 0.03	15.29 ± 0.02	1.19 ± 0.03	24.58 ± 0.23
F3	0.53 ± 0.02	0.65 ± 0.03	21.52 ± 0.02	1.27 ± 0.03	25.40 ± 0.21
F4	0.56 ± 0.03	0.60 ± 0.02	18.11 ± 0.03	1.22 ± 0.04	27.19 ± 0.21
F5	0.49 ± 0.04	0.63 ± 0.02	20.61 ± 0.04	1.15 ± 0.03	26.33 ± 0.22
F6	**0.50 ± 0.04**	**0.67 ± 0.02**	**25.32 ± 0.03**	**1.38 ± 0.03**	**24.44 ± 0.21**
F7	0.49 ± 0.03	0.55 ± 0.03	22.78 ± 0.03	1.39 ± 0.04	24.89 ± 0.18
F8	0.45 ± 0.03	0.69 ± 0.03	23.12 ± 0.02	1.29 ± 0.03	26.49 ± 0.11
F9	0.47 ± 0.03	0.53 ± 0.03	17.28 ± 0.02	1.14 ± 0.03	22.51 ± 0.23
F10	0.51 ± 0.02	0.64 ± 0.03	21.58 ± 0.02	1.15 ± 0.03	25.42 ± 0.21
F11	0.59 ± 0.03	0.69 ± 0.02	16.18 ± 0.03	1.29 ± 0.04	25.15 ± 0.21
F12	0.50 ± 0.04	0.59 ± 0.02	21.67 ± 0.04	1.24 ± 0.03	25.13 ± 0.22
F13	0.49 ± 0.04	0.70 ± 0.02	24.25 ± 0.03	1.39 ± 0.03	24.49 ± 0.21

3.14 Formulation of Tablet using Optimized ASDs

The optimized ASDs (F6) were selected for tablet formulation based on their superior solubility and dissolution performance. Tablets were prepared by incorporating the optimized ASDs equivalent to 250 mg of naproxen. The formulation compositions are presented in Table 19. The total tablet weight was maintained at 500 mg to ensure uniformity and ease of use. ASDs (325 mg) were used as the primary drug-containing component, whereas lactose (165 mg) was incorporated as a diluent to achieve the desired tablet weight and improve compressibility. Talc (5 mg) was added as a glidant to enhance the powder flow properties, and magnesium stearate (5 mg) was added as a lubricant to reduce friction during compression.

All ingredients were accurately weighed and blended uniformly to ensure a homogenous distribution of the drug within the formulation. The final blend exhibited satisfactory flow properties, facilitating uniform die filling and compression. The prepared tablets were subjected to evaluation parameters to assess their quality, performance, and drug release characteristics.

DOI: https://doi.org/10.66220/75p78209 ISSN: 3139-9258

Table 19. Formulation of Tablet containing ASDs

Sr. No.	Ingredients	Quantity
1	ASDs (F6) (Naproxen; 250mg Dose)	325mg
2	Lactose	165mg
3	Talc	5mg
4	Magnesium stearate	5mg
5	**Total Tablet Weight**	**500mg**

3.15 Evaluation of Tablets

The post-compression parameters of the optimized tablet formulation (F6 Tab) were evaluated to assess its quality, uniformity, and mechanical strength, as shown in Table 20. The hardness of the tablets was 4.9 ± 0.01 kg/cm², indicating adequate mechanical strength to withstand handling without compromising disintegration. The weight variation was within the acceptable pharmacopoeia limits (20 ± 2.31 mg), confirming uniformity in tablet weight and proper die filling during compression.

The thickness of the tablets was measured to be 3.1 ± 0.03 mm, demonstrating uniform tablet dimensions. The friability was 0.57 ± 0.02%, which is well below the acceptable limit of 1%, indicating good resistance to abrasion and mechanical stress. The drug content of the formulation was 99.85 ± 0.032%, confirming the uniform distribution of the drug within the tablets and compliance with standard limits.

Overall, the optimized formulation (F6 Tab) exhibited satisfactory post-compression characteristics, indicating its suitability for further in vitro dissolution and stability studies.

Table 20. Post-Compression Parameters of Tablets Formulation by SE (F6)

Batch Code	Hardness(kg/cm²)	Weight variation (mg)	Thickness (mm)	Friability (%)	% Drug content
F6 Tab	4.9 ± 0.01	20 ± 2.31	3.1 ± 0.03	0.57 ± 0.02	99.85 ± 0.032

3.15 *In-vitro* dissolution study

The *in-vitro* drug release profile of the F6 tablet demonstrated a progressive and efficient release pattern over 60 min. An initial slow release (9.86% at 10 min and 21.79% at 20 min) indicated the proper wetting and dissolution of the ASDs matrix. This is followed by a rapid release phase between 20 and 40 min (reaching 69.92%), suggesting enhanced solubility and reduced crystallinity due to the presence of PVP K30. The formulation achieved 96.23% drug release within 60 min, confirming almost complete drug availability. Low standard error values indicate good reproducibility. Overall, the F6 tablet showed improved dissolution behavior, likely due to ASDs formation, making it superior for enhancing the bioavailability of naproxen, as shown in Table 21 and Figure 24.

Table 21. *In-vitro* release profile of Tablets

Sr. No.	Time (Min.)	F6 Tab
1	0	0
2	10	9.86±0.04
3	20	21.79±0.03
4	30	54.29±0.02
5	40	69.92±0.09
6	50	85.09±0.03
7	60	96.23±0.01

DOI: https://doi.org/10.66220/75p78209 ISSN: 3139-9258

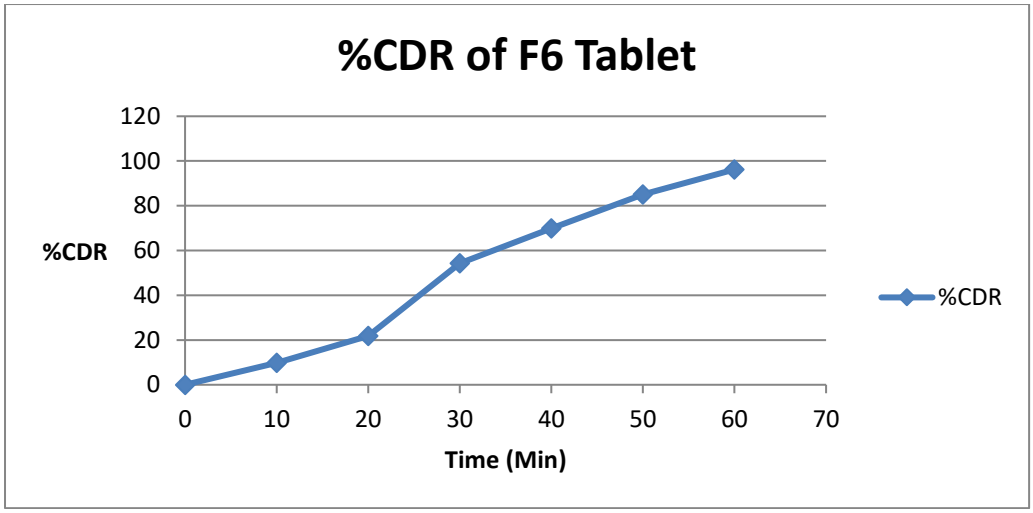


Figure 23. In-vitro drug release study F6 Tab

3.16 Kinetics of drug release

The kinetic study of the tablet formulation is presented in Table 22 and Figure 25, respectively. The results indicated that the F6 tablet formulation best followed the Korsmeyer–Peppas release kinetics model (R^2 = 0.9881), indicating the highest correlation among all models. Although the zero-order model (R^2 = 0.9784) also shows a good fit, the slightly higher R^2 value of the Peppas model confirms that the drug release mechanism is predominantly governed by non-Fickian diffusion, which involves both drug diffusion and polymer relaxation. The lower R^2 values observed for the first-order (0.8774) and Higuchi (0.8699) models suggest that the release is not purely concentration-dependent or diffusion-controlled. The Hixson–Crowell model (R^2 = 0.9503) indicates a minor contribution of matrix erosion. Overall, the F6 formulation demonstrated a controlled and anomalous drug release behavior, confirming the effectiveness of the ASDs system.

Table 22. R^2 values of various Kinetic Models

Kinetic Model	R^2 Value (F6 Tab)
Zero order	0.9784
First order	0.8774
Higuchi	0.8699
Hixon Crowell	0.9503
Korsemeyer Peppas	0.9881

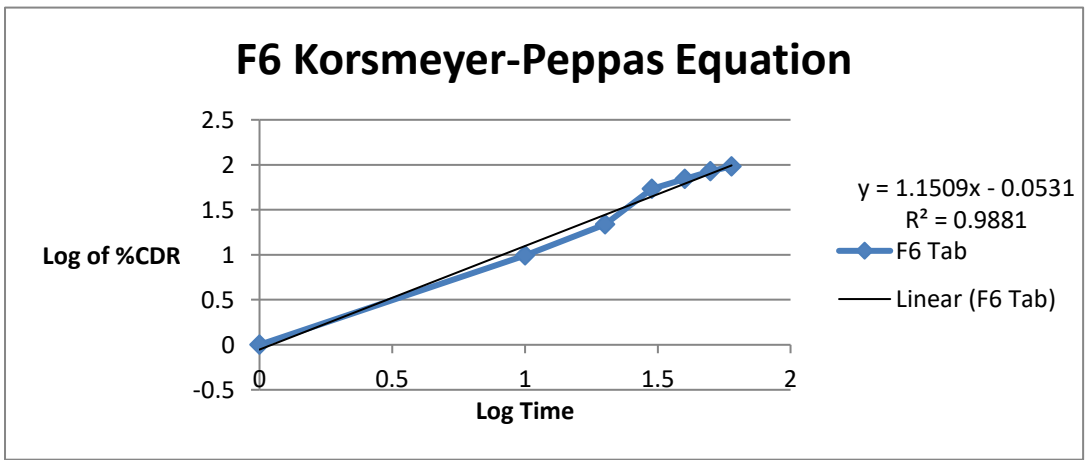


Figure 24. Kinetics of F6 Tab

3.17 Accelerated Stability Study

The optimized tablet formulation (F6) was subjected to accelerated stability studies under controlled temperature and humidity. The evaluated parameters included the thickness, hardness, and drug release over three months, as presented in Table 23. The thickness remained consistent within the range of 3.1 ± 0.04 to 3.2 ± 0.01 mm, indicating no significant dimensional variations. The hardness values showed minimal fluctuation (4.7 ± 0.04 to 4.9 ± 0.08 kg/cm²), confirming the retention of mechanical strength. The dissolution profile remained stable, with drug release ranging from 96.14 ± 0.09% to 96.96 ± 0.08%. Overall, no significant changes were observed in the evaluated parameters, demonstrating that F6 remained stable throughout the study period.

Table 23. Stability study of parameters of the optimized formulation (F6)

Parameters	Initial Month	1st Month	2nd Month	3rd Month
Thickness (mm)	3.1 ± 0.04	3.2 ± 0.02	3.1 ± 0.06	3.2 ± 0.01
Hardness	4.9 ± 0.03	4.8 ± 0.01	4.7 ± 0.04	4.9 ± 0.08
Dissolution (%)	96.23±0.01	96.58±0.07	96.14±0.09	96.96±0.08

4. Conclusion

In conclusion, this study demonstrates that the development of an amorphous solid dispersion (ASD)-based tablet is an effective formulation strategy for overcoming the poor aqueous solubility and dissolution limitations of naproxen. The optimized formulation exhibited desirable physicochemical characteristics, satisfactory tablet quality attributes, enhanced dissolution behavior, and acceptable stability under accelerated storage conditions, indicating the suitability of the selected formulation approach and hydrophilic polymer system. Systematic optimization using Response Surface Methodology (RSM) facilitated the identification of an optimum formulation with improved pharmaceutical performance while minimizing experimental variability. The findings of this study highlight the potential of amorphous solid dispersion technology as a simple, reproducible, and scalable approach for enhancing the performance of poorly water-soluble drugs. Therefore, the developed formulation may serve as a promising oral drug delivery system for naproxen, with the potential to improve therapeutic efficacy and patient compliance. Nevertheless, further in vivo pharmacokinetic and bioavailability studies followed by clinical evaluation are warranted to confirm the enhanced oral performance and therapeutic benefits of the optimized formulation.

Acknowledgments

None

Conflict of Interest

The authors declare no conflict of interest.

Authors' Contribution

Conceptualization; methodology; software; validation; formal analysis; investigation; resources; data curation; writing—original draft preparation; writing—review and editing; visualization; supervision; project administration by Parvez Musharraf Khan Ayyub Khan and Mohd Bilal Sufi. All authors have read and agreed to the published version of the manuscript.

Funding

This research received no external funding.

References

1. Aguiar ASN, Felimberti PZ, Duarte VS, Borges LL, Camargo AJ, Perjesi P, et al. Structural Studies of Sodium Counterion on Naproxen: From Solid State to Stability. Adv Phys Res. 2025;4(12). doi: 10.1002/apxr.202500159.

2. Kim H, Jang S, Kim IW. Enhanced dissolution of naproxen by combining cocrystallization and eutectic formation. Pharmaceutics. 2021;13(5). doi: 10.3390/pharmaceutics13050618.
3. Priyadarshinee S, Umamaheswari S, Ramesh M. Non-steroidal Anti-inflammatory Drug (NSAID) Naproxen-Induced Hepatotoxicity in a Freshwater Fish Labeo rohita. Water Air Soil Pollut. 2023;234(1). doi: 10.1007/s11270-022-06045-2.
4. Bárdos V, Szolláth R, Tőzsér P, Mirzahosseini A, Sinkó B, Angi R, et al. Study of the Influence of Pharmaceutical Excipients on the Solubility and Permeability of BCS Class II Drugs. Sci Pharm. 2025;93(2). doi: 10.3390/scipharm93020019.
5. Sievens-Figueroa L, Bhakay A, Jerez-Rozo JI, Pandya N, Romañach RJ, Michniak-Kohn B, et al. Preparation and characterization of hydroxypropyl methyl cellulose films containing stable BCS Class II drug nanoparticles for pharmaceutical applications. Int J Pharm. 2012;423(2):496–508. doi: 10.1016/j.ijpharm.2011.12.001.
6. Latif MS, Al-Harbi FF, Nawaz A, Rashid SA, Farid A, Mohaini M Al, et al. Formulation and Evaluation of Hydrophilic Polymer Based Methotrexate Patches: In Vitro and In Vivo Characterization. Polymers (Basel). 2022 Mar;14(7):1310. doi: 10.3390/polym14071310.
7. Hirun N, Kraisit P, Tantishaiyakul V. Thermosensitive Polymer Blend Composed of Poloxamer 407, Poloxamer 188 and Polycarbophil for the Use as Mucoadhesive In Situ Gel. Polymers (Basel). 2022;14(9). doi: 10.3390/polym14091836.
8. Veza I, Spraggon M, Fattah IMR, Idris M. Response surface methodology (RSM) for optimizing engine performance and emissions fueled with biofuel: Review of RSM for sustainability energy transition. Vol. 18, Results in Engineering. 2023. doi: 10.1016/j.rineng.2023.101213.
9. Myśliwiec P, Kubit A. Integrated multiobjective optimization of RFSSW parameters for AA2024-T3 using ANOVA machine learning and NSGA II. Sci Rep. 2025;15(1). doi: 10.1038/s41598-025-21941-3.
10. Reji M, Kumar R. Response surface methodology (RSM): An overview to analyze multivariate data. Vol. 9, Indian Journal of Microbiology Research. 2022. p. 241–8. doi: 10.18231/j.ijmr.2022.042.
11. Zhu Z, Li W, Yin Y, Cao R, Li Z. Differential Scanning Calorimetry Material Studies: Benzil Melting Point Method for Eliminating the Thermal History of DSC. Vol. 2022, Journal of Chemistry. 2022. doi: 10.1155/2022/3423429.
12. Arany D, Kőrösi M. Melting point depression of tetrabutylammonium halides in supercritical carbon dioxide. J Supercrit Fluids. 2025;223. doi: 10.1016/j.supflu.2025.106637.
13. Ndung S, Nyahanga T, Kinuthia E, Ndiritu A, Kirkok S, Kirimi J. Box-Behnken response surface methodology approach for rifampicin antibiotic fixed-bed optimization studies using macadamia nutshell activated carbon. J Chem Technol. 2025;1(4):173–88. doi: 10.22034/jchemtech.2025.543827.1020.
14. Siddiqui FA, Bakshi V. Hydroalcoholic Extraction, Phytoconstituent Profiling by LC-HRMS, and Computational Analysis of Lantana Camara as Potential Glucokinase, Alpha Amylase, Alpha Glucosidase, and DPP-IV Inhibitors. Chem Methodol. 2025;9(12):1189–220. doi: 10.48309/chemm.2025.532981.1980.
15. Shukla S, Kumar A, Pathak A, Kumar A, Tripathi K, Singh K. Green Synthesis of Benzimidazole Derivatives : A Sustainable Approach Towards Potent Antimicrobial Agents. J Chem Heal Risks. 2025;15(2):2634–49.
16. Mribha M, Sajan M, Ben B. Development and Characterization of Prednisolone Microspheres for the Treatment of Ulcerative Colitis. J Pharm Drug Deliv Res. 2024;13(1). doi: 10.4172/2325-9604.1000255.
17. Hess F, Kipping T, Weitschies W, Krause J. Understanding the Interaction of Thermal, Rheological, and Mechanical Parameters Critical for the Processability of Polyvinyl Alcohol-Based Systems during Hot Melt Extrusion. Pharmaceutics. 2024;16(4). doi: 10.3390/pharmaceutics16040472.
18. Abbood HK, Hateet RR. Isolation and identificatio of bacterium Pseudomonas aurginosa from burns and evaluation their ability to green synthesis of silver oxide nanoparticles as Antibacterial agent. Med Med Chem. 2024;1(3):129–37. doi: 10.22034/medmedchem.2024.491374.1021.
19. Olutayo O, Emmanuel Stella E, Omotola F. Biosynthesis of Iron Oxide Nanoparticles Using Moringa oleifera (Lam) Leaf Extract and Its Anti Plasmodial Studies. Chem Res Tech. 2025;2:99–107. doi: 10.22034/CHEMRESTEC.2025.514186.1043.

20. Bhosale PM, Singh M. Optimizing Pharmaceutical Formulations: Advancements in Nanosuspension Pre-Formulation to Enhance Solubility and Bioavailability of Active Agents. Int J Membr Sci Technol. 2023;10(5):804–12. doi: 10.15379/ijmst.v10i5.3546.
21. Zampieri FG, Cansian Junior JC, Rodrigues VAP, Lambert JC, Souza T da S de, Oliveira A de FM de, et al. Evaluation of the chemical composition and quantification of capsaicin in oleoresin from peppers of the genus Capsicum spp. DELOS Desarro Local Sosten. 2024;17(54):e1380. 10.55905/rdelosv17.n54-002.
22. Sawant MP, Deokar GS. Solubility Profiling and UV-Spectrophotometric Determination of Bioactive Peptides from Ragi. Int J Drug Deliv Technol. 2025;15(3):1265–71. doi: 10.25258/ijddt.15.3.47.
23. Muhtadi WK, Firmansyah F, Agustini TT, Rahayu P, Fitriyanti SA, Ulfa R. Validation of Spectrophotometric Method To Quantify Quercetin in the in Vitro Dissolution Study of Self Nano-Emulsifying Drug Delivery System (Snedds). J Farm Sains dan Prakt. 2022;268–73. doi: 10.31603/pharmacy.v8i3.6258.
24. Higuchi T, Shih FL, Kimura T, Rytting JH. Solubility determination of barely aqueous-soluble organic solids. J Pharm Sci. 1979;68(10):1267–72. doi: 10.1002/jps.2600681019.
25. Ramadhan S, Omer H. The development of ternary and quaternary ASDs based hydrotropic blends of atorvastatin calcium. Zanco J Med Sci. 2024;28(1):95–110. doi: 10.15218/zjms.2024.010.
26. Zhao T, Gu C, Qi J, Liu J, Wang Y, Chen X, et al. In vitro and in vivo performance of ASDs of ursolic acid as a function of polymer type and excipient addition. J Pharm Pharmacol. 2024;76(12):1584–98. doi: 10.1093/jpp/rgae125.
27. Krzak A, Bilewicz R. Voltammetric/UV–Vis study of temozolomide inclusion complexes with cyclodextrin derivatives. Bioelectrochemistry. 2020;136. doi: 10.1016/j.bioelechem.2020.107587.
28. Sherje AP, Londhe V. Ternary Inclusion Complex of Paliperidone with β-Cyclodextrin and Hydrophilic Polymer for Solubility and Dissolution Enhancement. J Pharm Innov. 2015;10(4):324–34.
29. AlQasas N, Johnson D. Determination of Hansen solubility parameters of water-soluble proteins using UV–vis spectrophotometry. Heliyon. 2023;9(11). 10.1016/j.heliyon.2023.e21403.
30. Naureen F, Shah Y, Shahnaz, Khuda F. Determination of Saturated Solubility of Mirtazapine Using UV Visible Spectrophotometer. Pharm Commun. 2024;3(1):27–34. doi: 10.55627/pharma.003.001.0799.
31. Syed MA, Nahida S. Effect of Sonication on Solubility of Posaconazole in Different Solvents. J PharmTechNova. 2026;01(01):42–8. doi: 10.66220/vagg1j45.
32. Podder S, Mukherjee S. Response Surface Methodology (Rsm) As a Tool in Pharmaceutical Formulation Development. Asian J Pharm Clin Res. 2024;17(11):18–25. doi: 10.22159/ajpcr.2024v17i11.52149.
33. Alalaiwe A, Alsenaidy MA, Almalki ZS, Fayed MH. Development and Optimization of Sildenafil Orodispersible Mini-Tablets (ODMTs) for Treatment of Pediatric Pulmonary Hypertension Using Response Surface Methodology. Pharmaceutics. 2023;15(3). doi: 10.3390/pharmaceutics15030923.
34. Al-Asadi LJAS, Al-Edresi S. Reduction of Time and Cost in Preparation of Nanofibers From Pva, Peo and Hpmc Using Design-Expert® Software. Int J Appl Pharm. 2024;16(4):257–66. doi: 10.22159/ijap.2024v16i4.50022.
35. Ulvi H, Yerlikaya MA, Yildiz K. Urban Traffic Mobility Optimization Model: A Novel Mathematical Approach for Predictive Urban Traffic Analysis. Appl Sci. 2024;14(13). doi: 10.3390/app14135873.
36. Andrew E, Chidera A, Ekemezie O, Pauline O, Chinedu N, Godswill O. Preparation and Evaluation of Ranitidine Hydrochloride Floating Microspheres. Am J Polym Sci Technol. 2024;10(2):36–46. doi: 10.11648/j.ajpst.20241002.12.
37. Anusha V, Umashankar MS, Ganesh Kumar Y. Preformulation Studies of Pitavastatin Calcium– A Primary Step in Further Design of Chronotherapeutic Formulation Synchronized with Circadian Rhythm. Int J Drug Deliv Technol. 2024;14(3):1578–85. doi: 10.25258/ijddt.14.3.46.
38. Harahap FS, Oesman R, Fadhillah W, Nasution AP. Penentuan Bulk Density Ultisol Di Lahan Praktek Terbuka Universitas Labuhanbatu. AGROVITAL J Ilmu Pertan. 2021;6(2):56. doi: 10.35329/agrovital.v6i2.1913.
39. Daharwal SJ, Prakash Rao S, Singh VK, Chandrakar K, Singh VD. Formulation and characterization of metformin HCl sustained release matrix tablet by using Cassia tora mucilage. Res J Pharm Technol. 2015;8(7):871–9. doi: 10.22270/jddt.v7i6.1520.

40. Phanapithakkun S, Yusakul G, Sitthisak C, Plyduang T. Development of tablet formulations containing genistein ASDs optimized using Box-Behnken design for enhanced solubility. J Appl Pharm Sci. 2025;15(4):53–64. doi: 10.7324/japs.2025.222224.
41. Bunlung S, Nualnoi T, Issarachot O, Wiwattanapatapee R. Development of raft-forming liquid and chewable tablet formulations incorporating quercetin ASDs for treatment of gastric ulcers. Saudi Pharm J. 2021;29(10):1143–54. doi: 10.1016/j.jsps.2021.08.005.
42. El-Helaly SN, Rashad AA. Mirtazapine loaded polymeric micelles for rapid release tablet: A novel formulation—In vitro and in vivo studies. Drug Deliv Transl Res. 2024;14(9):2488–98. doi: 10.1007/s13346-024-01525-w.
43. Ali EA, Ahmed OS, Shokri H. A Comparative Quality Study of Selected Authorized and Smuggled Medicines in Aden, Yemen. Electron J Univ Aden Basic Appl Sci. 2023;4(2):178–86. doi: 10.47372/ejua-ba.2023.2.249.
44. Zhu W, Long J, Shi M. Release Kinetics Model Fitting of Drugs with Different Structures from Viscose Fabric. Materials (Basel). 2023;16(8). doi: 10.3390/ma16083282.
45. Askarizadeh M, Esfandiari N, Honarvar B, Sajadian SA, Azdarpour A. Kinetic Modeling to Explain the Release of Medicine from Drug Delivery Systems. ChemBioEng Rev. 2023;10(6):1006–49. doi: 10.1002/cben.202300027.